Theory of Quantum Condensed Matter - Introduction to the theory of correlated many-body quantum systems -

Master Concepts Fondamentaux de la Physique
Sep-Dec 2014

Antoine Georges, with Xavier Leyronas and Christophe Mora

September 29, 2014

Contents

Chapter 1

The Bose-Hubbard model and the superfluid to Mott insulator transition

In this section, we make our first encounter with the Mott phenomenon: strong repulsive interactions between particles can prevent the formation of an itinerant state and favour a situation in which particles are localized. This phenomenon is of key importance to the physics of strongly correlated materials. Many remarkable physical properties are found for those materials which are close to a Mott insulating state. For example, high-temperature superconductivity is found in copper oxides when a metallic state is induced by introducing a relatively small amount of charge carriers into a Mott insulator.

In such circumstances, particles "hesitate" between itinerant and localized behaviour, making quantum coherence more difficult to establish and leading to a number of possible instabilities. From a theoretical viewpoint, one of the key difficulties is to describe consistently an entity which is behaving simultaneously in a wave-like (delocalized) and particle-like (localized) manner. Viewed from this perspective, strongly correlated quantum systems raise fundamental questions in quantum physics. Because the Mott phenomenon is so important, the theoretical proposal [**?**] and experimental observation [**?**] of the Mott transition in a gas of ultra-cold bosonic atoms in an optical lattice have truly been pioneering works establishing a bridge between modern issues in condensed matter physics and ultra-cold atomic systems.

In this section, we deal with this phenomenon in the simplest possible

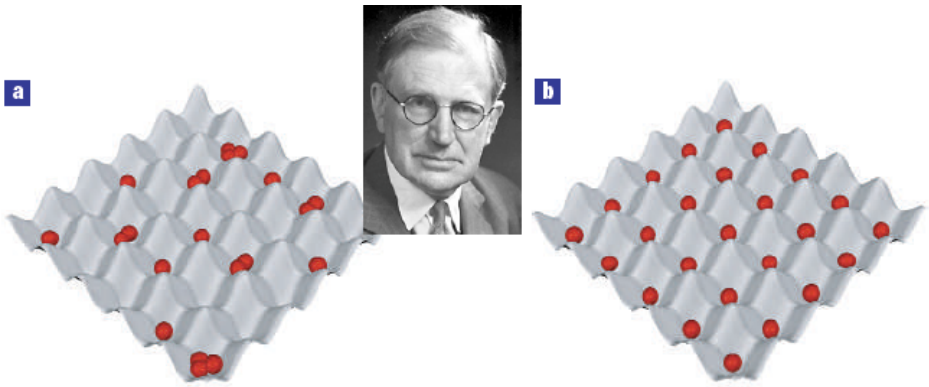

Figure 1.1: (a) Typical real-space configuration of particles in an itinerant (metallic or superfluid) state. (b) Typical real-space configuration in the Mott insulating state, in which double-occupancies are strongly suppressed. (Center:) Sir Nevil Mott. Adapted in part from [**?**].

context: that of the Hubbard model for bosonic atoms in an optical lattice. The case of fermions will be considered later, in Secs.5,**??**. The hamiltonian of this model reads:

$$H = -\sum_{ij} t_{ij}\, b_i^\dagger b_j + \frac{U}{2}\sum_i \hat{n}_i(\hat{n}_i - 1) + \sum_i v_{\rm trap}(i)\,\hat{n}_i - \mu \sum_i \hat{n}_i$$

1.1 General considerations: lifting a macroscopic degeneracy

Let us first consider a homogeneous system ($v_{\rm trap} = 0$) in the limit where there is no hopping $t_{ij} = 0$ (very deep lattice). In condensed-matter physics, this limit is called the "atomic limit", referring to the solid as a collection of identical atoms. The hamiltonian is then diagonal in occupation-number basis and has eigenstates $|n\rangle$ with energies $E_n^0 = \frac{U}{2}n(n-1) - \mu n$. These energy levels cross at specific values of the chemical potential $\mu_n^0 = nU$ at which $E_n^0 = E_{n+1}^0$. Hence, the nature of the ground-state depends crucially on the value of the chemical potential:

- If $\mu \in](n-1)U, nU[$, the ground-state is *non-degenerate*, with exactly n bosons on each lattice site.

- If $\mu = nU$, having n or $n-1$ bosons on each lattice site is equally probable. Hence, the ground-state has a *macroscopic degeneracy* 2^{N_s} (with N_s the number of sites in the lattice).

The number of particles per site in the ground-state as a function of chemical potential has the form of a "staircase" made of plateaus of width U in which $\langle \hat{n} \rangle$ remains constant, separated by steps at $\mu_n^0 = \mu n$ at which it jumps by one unit (Fig. 1.2). In the context of mesoscopic solid-state devices, this is called the "Coulomb staircase": in order to increase the charge by one unit, a Coulomb charging energy must be paid due to the electrostatic repulsive interactions between electrons.

Within a given plateau $\mu \in](n-1)U, nU[$, the first excited state (at constant total particle number) consists in moving one boson from one site to another one, leaving a site with occupancy $n-1$ and another one with occupancy $n+1$. The energy of this excitation is:

$$\Delta_g^0 = E_{n+1}^0 + E_{n-1}^0 - 2E_n^0 = U \tag{1.1}$$

Hence, the ground-state is separated from the first excited state by a *finite energy gap*. (In passing, we note that this gap can be written as $\Delta_g^0 = (E_{n+1}^0 - E_n^0) + (E_{n-1}^0 - E_n^0)$ which in chemist's terminology corresponds to ionization energy minus affinity). Adding or removing an electron also requires a finite amount of energy: hence the system is *incompressible*. Indeed, each plateau has a vanishing compressibility:

$$\kappa = \left(\frac{\partial^2 E}{\partial n^2} \right)^{-1} = \frac{\partial n}{\partial \mu} \tag{1.2}$$

Having understood the zero-hopping limit, we can ask what happens when a small hopping amplitude is turned on. Obviously, a non-degenerate incompressible ground-state separated by a gap from all excitations is a quite protected state. Hence, we expect that the system will remain incompressible and localized when turning on a small hopping, for μ well within a given charge plateau. In contrast, the hopping amplitude is likely to be a singular perturbation when starting from the macroscopically degenerate ground-state at each of the degeneracy points $\mu_n^0 = nU$. One natural way for the perturbation to lift the degeneracy is to select a unique ground-state which is a superposition of the different degenerate configurations, with different number of particles on each site. If the mixing between the different charge states corresponds to a state with small phase fluctuations (the phase is the conjugate variables to the local charge), the resulting state will be a

superfluid. Hence, we expect that a superfluid state with Bose condensation will occur already for infinitesimal hopping at the degeneracy points $\mu = nU$. These expectations are entirely confirmed by the mean-field theory presented in the next section. We note in passing that interesting phenomena often happen in condensed-matter physics when a perturbation lifts a large degeneracy of the ground-state (the fractional quantum Hall effect is another example).

1.2 Mean-field theory of the bosonic Hubbard model

As usually the case in statistical mechanics, a mean-field theory can be constructed by replacing the original hamiltonian on the lattice by an effective single-site problem subject to a self-consistency condition. Here, this is naturally achieved by factorizing the hopping term [**?**, **?**]: $b_i^\dagger b_j \to \text{const.} + \langle b_i^\dagger \rangle b_j + b_i^\dagger \langle b_j \rangle + \cdots$ in which "$\cdots$" denote fluctuations which are neglected. Another essentially equivalent formulation is based on the Gutzwiller wavefunction [**?**, **?**]. The effective 1-site hamiltonian for site i reads:

$$h_{\text{eff}}^{(i)} = -\lambda_i b^\dagger - \lambda_i b + \frac{U}{2}\hat{n}(\hat{n}-1) - \mu\hat{n} \tag{1.3}$$

In this expression, λ_i is a "Weiss field" which is determined self-consistently by the boson amplitude on the other sites of the lattice through the condition:

$$\lambda_i = \sum_j t_{ij} \langle b_j \rangle \tag{1.4}$$

For nearest-neighbour hopping on a uniform lattice of connectivity z, with all sites being equivalent, this reads:

$$\lambda = z\, t \langle b \rangle \tag{1.5}$$

These equations are easily solved numerically, by diagonalizing the effective single-site hamiltonian (1.3), calculating $\langle b \rangle$ and iterating the procedure such that (1.5) is satisfied. The boson amplitude $\langle b \rangle$ is an order-parameter associated with Bose condensation in the $\vec{k} = 0$ state: it is non-zero in the superfluid phase.

For densities corresponding to an integer number n of bosons per site on average, one finds that $\langle b \rangle$ is non-zero only when t/U is larger than a critical ratio $(t/U)_c$ (which depends on the filling n). For $t/U < (t/U)_c$, $\langle b \rangle$ (and λ) vanishes, signalling a non-superfluid phase in which the bosons are localised on the lattice sites: the Mott insulator. For non-integer values of

the density, the system is a superfluid for all $t/U > 0$. This fully confirms the expectations deduced on a qualitative basis at the end of the previous section.

1.2.1 Perturbative analysis

It is instructive to analyze these mean-field equations close to the critical value of the coupling: because λ is then small, it can be treated in (1.3) as a perturbation of the zero-hopping hamiltonian . Considering a given plateau $\mu \in](n-1)U, nU[$, the perturbed ground-state reads:

$$|\psi_0\rangle = |n\rangle - \lambda \left[\frac{\sqrt{n}}{U(n-1)-\mu}|n-1\rangle + \frac{\sqrt{n+1}}{\mu - Un}|n+1\rangle \right] \tag{1.6}$$

so that:

$$\langle\psi_0|b|\psi_0\rangle = -\lambda \left[\frac{n}{U(n-1)-\mu} + \frac{n+1}{\mu - Un} \right] \tag{1.7}$$

Inserting this in the self-consistency condition yields:

$$\lambda = -z\,t\,\lambda \left[\frac{n}{U(n-1)-\mu} + \frac{n+1}{\mu - Un} \right] + \cdots \tag{1.8}$$

where "..." denotes higher order terms in λ. This equation can be viewed as the linear term in the expansion of the equation of state for λ. As usual, the critical value of the coupling corresponds to the vanishing of the coefficient of this linear term (corresponding to the quadratic or mass term of the expansion of the Landau free-energy). Hence the critical boundary for a fixed average (integer) density n is given by:

$$\frac{zt}{U} = \frac{(n-\mu/U)(\mu/U-n+1)}{1+\mu/U} \tag{1.9}$$

1.2.2 Phase diagram.

This expression gives the location of the critical boundary as a function of the chemical potential. As expected, it vanishes at the degeneracy points $\mu_n^0 = nU$ where the system becomes a superfluid for infinitesimal hopping amplitude. In the $(t/U, \mu/U)$ plane, the phase diagram (Fig. 1.2) consists of lobes inside which the density is integer and the system is a Mott insulator. Outside these lobes, the system is a superfluid. The tip of a given lobe

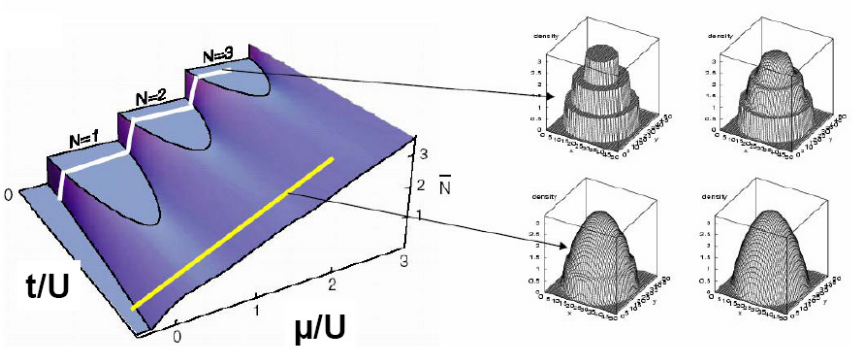

Figure 1.2: Left: phase diagram of the Bose Hubbard model as a function of chemical potential μ/U and coupling t/U. An incompressible Mott insulator is found within each lobe of integer density. Right: density profiles in a harmonic trap. The "wedding cake" structure (see text) is due to the incompressibility of the Mott insulator (numerical calculations courtesy of H.Niemeyer and H.Monien, figure courtesy F.Gerbier).

corresponds to the the maximum value of the hopping at which an insulating state can be found. For n atoms per site, this is given by:

$$\frac{zt}{U}|_{c,n} = \mathrm{Max}_{x\in[n-1,n]}\frac{(n-x)[x-n+1]}{1+x} = \frac{1}{2n+1+2\sqrt{n(n+1)}} \qquad (1.10)$$

So that the critical interaction strength is $(U/zt)_c \simeq 5.8$ for $n = 1$, and increases as n increases ($(U/zt)_c \sim 4n$ for large n).

1.2.3 Mott gap.

The gap in the Mott insulating state is of course reduced by the hopping from its zero-hopping value $\Delta_g^0 = U$. We can obtain its mean-field value from the extension of the density plateau:

$$\Delta_g(n) = \mu_+(n) - \mu_-(n) \qquad (1.11)$$

where $\mu_\pm$ are the solutions of the quadratic equation corresponding to (1.9), i.e:

$$(\mu/U)^2 - [2n-1-(zt/U)](\mu/U) + n(n-1) + (zt/U) = 0 \qquad (1.12)$$

yielding:

$$\Delta_g(n) = U\left[(\frac{zt}{U})^2 - 2(2n+1)\frac{zt}{U} + 1\right]^{1/2} \tag{1.13}$$

The Mott gap is $\sim U$ at large U/t and vanishes at the critical coupling ($\propto (U-U_c)^{1/2}$ within mean-field theory).

1.2.4 Incompressibility and "wedding-cake" shape of the density profile in the trap

The existence of a gap means that the chemical potential can be changed within the gap without changing the density. As a result, when the system is placed in a trap, it displays density plateaus corresponding to the Mott state, leading to a "wedding cake" structure of the density profile (Fig. 1.2). This is easily understood in the local density approximation, in which the local chemical potential is given by: $\mu(r) = \mu - v_{\rm trap}(r) = \mu - m\omega_0^2 r^2/2$, yielding a maximum extension of the plateau: $\sim (2\Delta_g/m\omega_0^2)^{1/2}$. Several authors have studied these density plateaus beyond the LDA by numerical simulation (see e.g [**?**]), and they have also been imaged experimentally, see e.g. [**?**].

1.3 Mean-field theory: the wave-function viewpoint

An alternative, but equivalent, viewpoint on the above mean-field theory is to formulate it as a variational ansatz for the ground-state wave-function [**?**, **?**].

In the zero-hopping limit, the ground-state wave-function within a given density plateau reads:

$$\Psi_0^{t=0} = \prod_i |n\rangle_i = \prod_i \frac{1}{\sqrt{n!}}(b_i^\dagger)^n|0\rangle \tag{1.14}$$

In the opposite limit of a non-interacting system ($U=0$), the ground-state wave-function is obtained by placing all bosons in the $\vec{k}=0$ state:

$$\Psi_0^{U=0} = \frac{1}{\sqrt{N!}}(b_{\vec{k}=0}^\dagger)^N|0\rangle = \frac{1}{\sqrt{N!}}\left[\frac{1}{\sqrt{N_s}}\sum_i b_i^\dagger\right]^N|0\rangle \tag{1.15}$$

In the limit of large N, N_s, the ground-state wavefunction for the non-interacting case can alternatively be formulated (by letting N fluctuate)

as a product of coherent states on each site:

$$\Psi_0^{U=0} = \prod_i |\alpha\rangle_i \ , \ \ |\alpha\rangle = e^{-|\alpha|^2/2} \sum_{n=0}^{\infty} \frac{\alpha^n}{\sqrt{n!}} |n\rangle \tag{1.16}$$

with $|\alpha|^2 = \langle n \rangle = N/N_s$. In this limit, the local density obeys Poisonnian statistics $p(n) = e^{-|\alpha|^2} |\alpha|^{2n}/n! = e^{-\langle n \rangle} \langle n \rangle^n / n!$.

We note that in both limits, the ground-state wave-function is a product of individual wave-functions over the different lattice sites. The individual wave-functions have a very different nature however in each limit: they are number state for $t = 0$ while they are a phase-coherent superposition of number states in the $U = 0$ limit.

A natural variational ansatz is then to assume that the wave-functions remains an uncorrelated product over sites for arbitrary U/t, namely:

$$\Psi_0^{\rm var} = \prod_i \left[\sum_n c_n |n\rangle_i \right] \tag{1.17}$$

The variational principle then leads to equation for the coefficients c_n which are identical to the mean-field equations above. The trial wave-function interpolates between the Poissonian statistics $c_n = \alpha^n/\sqrt{n!}$ for $U = 0$ and the zero-fluctuation limit $c_n = \delta_{n,n_0}$ as the insulator is reached. The fact that n has no fluctuations throughout the Mott phase is of course an artefact of the mean-field.

1.4 Relation with the quantum XY model

1.5 Beyond mean-field: universal critical behaviour at the Mott transition

Chapter 2

Introduction to fermions

2.1 Models

2.1.1 The single-level 'Hubbard' atom

$$\hat{H}_{at} = \varepsilon_d(\hat{n}_\uparrow + \hat{n}_\downarrow) + U\hat{n}_\uparrow\hat{n}_\downarrow \tag{2.1}$$

Four eigenstates:

- $|0\rangle$ Energy: 0, ground-state for $\varepsilon_d > 0$
- $|\uparrow\rangle, |\downarrow\rangle$ Energy: ε_d Doubly-degenerate ground-state for $-U < \varepsilon_d < 0$
- $|\uparrow\downarrow\rangle$ Energy: $2\varepsilon_d + U$. Ground-state for $\varepsilon_d < -U$.

Level crossings at $\varepsilon_d = 0$ and $\varepsilon_d = -U$. At these points, one has an extra degeneracy of two ground-states with occupancies differing by one unit.

Occupancy (charge) as a function of position of d-level, at finite temperature. Grand-canonical partition function:

$$Z \;=\; 1 + 2e^{-\beta\varepsilon_d} + e^{-\beta(2\varepsilon_d+U)} \tag{2.2}$$

Boltzmann weights of $0\rangle$, $|\sigma\rangle$ and $\uparrow\downarrow\rangle$, respectively: $1/Z$, $e^{-\beta\varepsilon_d}/Z$, $e^{-\beta(2\varepsilon_d+U)}/Z$. Hence:

$$\langle\hat{n}_\sigma\rangle \;=\; \frac{e^{-\beta\varepsilon_d} + e^{-\beta(2\varepsilon_d+U)}}{1 + 2e^{-\beta\varepsilon_d} + e^{-\beta(2\varepsilon_d+U)}} \tag{2.3}$$

This is the 'Coulomb staircase', describing the Coulomb blockade by the repulsive interaction.

[PLOT]

Particle-hole symmetry For the special value $\varepsilon_d = -U/2$, the above spectrum has an extra degeneracy: the empty state $|0\rangle$ and fully occupied state $|\uparrow\downarrow\rangle$ are degenerate ($2\varepsilon_d + U = 0$). The Coulomb staircase above is also obviously symmetric with respect to this value.

It is easily checked that in this case, the atomic hamiltonian has the following symmetry, which exchanges particles and holes:

$$d_\sigma \to d_\sigma^\dagger \ , \ \ d_\sigma^\dagger \to d_\sigma \tag{2.4}$$

Indeed, under this transformation:

$$\hat{n}_\sigma \to 1 - \hat{n}_\sigma \tag{2.5}$$

so that:

$$\hat{H}_{at} \to (2\varepsilon_d + U) - (\varepsilon_d + U) \sum_\sigma \hat{n}_\sigma + U \hat{n}_\uparrow \hat{n}_\downarrow \tag{2.6}$$

Hence, for $\varepsilon_d = -(\varepsilon_d + U)$, the atomic hamiltonian is left invariant.

A more in-depth discussion of the symmetries of the Hubbard model will be given below.

2.1.2 Atom in a bath: from magnetic impurities to quantum dots

Anderson (-Wolf) model of a single magnetic impurity atom in a metallic host (e.g. Cu:Mn). The host is modelled as a free electrons and can exchange electrons with the impurity atom.

$$H_{\rm AIM} \ = \sum_{\mathbf{k}\sigma} \varepsilon_{\mathbf{k}} \, c_{\mathbf{k}\sigma}^\dagger c_{\mathbf{k}\sigma} + H_{at}^d + \sum_{\mathbf{k}\sigma} (V_{\mathbf{k}} d_\sigma^\dagger c_{\mathbf{k}\sigma} + h.c.) \tag{2.7}$$

A slight variation of this model allowing for more than one electronic bath also describes the physics of a single electronic level of a quantum dot, coupled to reservoirs (electrodes). The AIM has received a renewal of interest starting in the late 1990's in this context.

[FIGURE ?]

2.1.3 The periodic Anderson model: heavy-fermion compounds

The so-called heavy-fermion compounds (for example, $CeAl_3$) involve elements with very localized atomic orbitals, typically the f-shell of a rare-earth or actinide element. The compound involves as well a lighter element with

delocalized conduction-electron orbitals. The two (or more) elements occupy distinct sites of a periodic crystal lattice.

The simplest model describing this situation is a periodic (translationally invariant) generalization of the Anderson impurity model:

$$H_{\rm PAM} \;=\; \sum_{\mathbf{k}\sigma} \varepsilon_{\mathbf{k}}\, c^\dagger_{\mathbf{k}\sigma} c_{\mathbf{k}\sigma} + \sum_i \Big[\varepsilon_f(\hat{n}^f_{i\uparrow}+\hat{n}^f_{i\downarrow}) + U\hat{n}^f_{i\uparrow}\hat{n}^f_{i\downarrow}\Big] + \sum_{\mathbf{k}\sigma}(V_{\mathbf{k}} f^\dagger_{\mathbf{k}\sigma} c_{\mathbf{k}\sigma} + \text{h.c.}) \tag{2.8}$$

Exercise: Work out the bandstructure of this hamiltonian for $U = 0$. Explain the notion of 'hybridization gap'. What is the physical state of the system in the particle-hole symmetric case $\varepsilon_f = 0$ and what is the values of the occupancies n_c, n_f then ? In contrast, what happens when $\varepsilon_f \neq 0$?

2.1.4 The Hubbard model: narrow bands and transition-metal oxides

Consider a lattice of single-level Hubbard-like atoms, coupled together by single-particle hopping:

$$H \;=\; -\sum_{ij\sigma} t_{ij}\, d^\dagger_{i\sigma} d_{j\sigma} \;+\; U \sum_i \hat{n}_{i\uparrow}\hat{n}_{i\downarrow} \tag{2.9}$$

This model is the simplest model of correlated electrons (simplest to formulate, not to solve !). It plays in this field a role somewhat similar to that of the Ising model in classical statistical mechanics and magnetism. It is the model of choice to describe a narrow electronic band subject to a Coulomb which is screened well enough that the non-local matrix elements of teh Coulomb interaction can be neglected.

Historically, it was introduced as a model for itinerant ferromagnetism in the narrow d-band of transition metals. In the past 30 years or so however, with the flurry of interest in copper-oxide high-T_c superconductors, it has been mostly discussed as an effective model for transition-metal oxides and their Mott insulator to metal transition.

The electronic structure of an oxide is obviously more complex however: it includes both oxygen p and metal d-orbitals, and a minimal model should rather be:

$$H \;=\; -\sum_{\langle ij\rangle\sigma} t_{pd}\, \Big[d^\dagger_{i\sigma} p_{j\sigma} + p^\dagger_{j\sigma} d_{i\sigma}\Big] + \varepsilon_p \sum_{i\sigma} p^\dagger_{i\sigma} p_{i\sigma} + \varepsilon_d \sum_{i\sigma} d^\dagger_{i\sigma} d_{i\sigma} + U\sum_i \hat{n}^d_{i\uparrow}\hat{n}^d_{i\downarrow} \tag{2.10}$$

in which the lattice (e.g. a perovskite lattice) has two kinds of sites carrying each type of atoms. A key parameter in this hamiltonian is the difference

between the on-site energies of oxygen and metal orbitals, $\Delta \equiv \varepsilon_d - \varepsilon_p$, called the *charge-transfer energy*. In transition-metal oxides involving elements of the early part of the transition-metal row, this energy is very large: $\Delta \gg U \gg t_{pd}$. In this limit, the oxygen orbitals are fully filled (corresponding to the ionization configuration O^{2-} of oxygen, and the oxygen orbitals can be eliminated to yield an effective model for transition-metal orbitals only. This model is a single-band Hubbard model, with an effective hopping which reads (to second order in perturbation theory in t_{pd}/Δ:

$$t_{\text{eff}} \propto \frac{t_{pd}^2}{\Delta} \tag{2.11}$$

For oxides involving transition-metals with larger atomic number Z however, this is no longer true and oxygen orbitals cannot be eliminated so simply at low-energy. In extreme cases, the oxygen valence may not be quite O^{2-} and holes may appear in ligand orbitals. The distinction between early and late transition metal-oxides is the basis of the Zaanen-Sawatzky-Allen classification [REF].

2.2 Strong coupling and superexchange

The isolated Hubbard atom for $-U < \varepsilon_d < 0$ has a doubly degenerate ground-state. For the AIM, this raises the interesting and important question of what happens when a hybridization to a bath is turned on, starting from this limit. For the Hubbard model, this means that the ground-state at half-filling for zero hopping has a macroscopic 2^N degeneracy: how is this degeneracy lifted when a small non-zero hopping is turned on ? The two other regimes (empty orbital $\varepsilon_d \gg 0$ and doubly occupied case $\varepsilon_d \ll -U$) are far less interesting. The 'mixed valence' regimes $\varepsilon_d \simeq -U$ and $\varepsilon_d \simeq 0$) raise interesting question too, with an even larger degeneracy in the atomic limit.

To answer this question, it is a very useful to treat a simple two-site model by exact diagonalisation. For the AIM: a single conduction orbital hybridized to the atomic site. For the Hubbard model: a two-site model. We specialize these models to the case of particle-hole symmetry, for simplicity:

$$H_{\text{AIM1}} = U \left(\hat{n}_\uparrow - \frac{1}{2}\right)\left(\hat{n}_\downarrow - \frac{1}{2}\right) + V \sum_\sigma (d_\sigma^\dagger c_\sigma + c_\sigma^\dagger d_\sigma) \tag{2.12}$$

$$H_{H2} = \sum_{i=1}^{2} U \left(\hat{n}_{i\uparrow} - \frac{1}{2}\right)\left(\hat{n}_{i\downarrow} - \frac{1}{2}\right) - t \sum_\sigma (d_{1\sigma}^\dagger d_{2\sigma} + d_{2\sigma}^\dagger d_{1\sigma}) \tag{2.13}$$

We observe that these models conserve:

- The *total* particle number $N = n_c + n_d$ or $N = n_{d1} + n_{d2}$ ($U(1)$ symmetry)
- The *total spin* S and S_z ($SU(2)_s$ symmetry)

Hence the total Hilbert space factors out into:

$$2^4 = 16 = 1 + (2+2) + (3+3) + (2+2) + 1 \tag{2.14}$$

groups of states, corresponding to:

$$\begin{aligned}(N=0,S=0) \oplus (N=1,S_z=-1/2) \oplus (N=2,S_z=+1/2) \oplus (N=2,S=1) \oplus (N=2,S=0) \\ \oplus (N=3,S_z=-1/2) \oplus (N=3,S_z=+1/2) \oplus (N=4,S=0)\end{aligned} \tag{2.15}$$

We consider the sector with one particle per site on average ($N = 2$, 6 states), which splits into a triplet sector $S = 1$ (3 states) and a singlet sector ($S = 0$, 3 states too since there are two sites).

The triplet sector is unaffected by the hopping. *Exercise: check this !.*

In the singlet sector, we have the following matrix for the AIM1 hamiltonian, ordering states as : $|\uparrow\downarrow,0\rangle, |\uparrow,\downarrow\rangle_{S=0}, |0,\uparrow\downarrow\rangle$

$$\begin{pmatrix} U/4 & V\sqrt{2} & 0 \\ V\sqrt{2} & -U/4 & V\sqrt{2} \\ 0 & V\sqrt{2} & U/4 \end{pmatrix} \tag{2.16}$$

Eigenvalues are solution of:

$$(U/4 - E)\left[E^2 - \frac{U^2}{16} - 4V^2\right] = 0 \tag{2.17}$$

$$E = \frac{U}{4} \;\; ; \;\; E_\pm = \pm\frac{U}{4}\sqrt{1 + \frac{64V^2}{U^2}} \tag{2.18}$$

The ground-state is now non-degenerate and belongs to the singlet sector. For small $V \ll U$, it is essentially the state $|\uparrow,\downarrow\rangle_{S=0}$ with a small admixture (of order V/U) of the two other (doubly occupied) states. The lowering of energy as compared to the value for $V = 0$ (and to the triplet sector) is, for $V \ll U$, since $E_- \simeq -U/4 - 8V^2/U + \cdots$

$$J_K = \frac{8V^2}{U} \tag{2.19}$$

Separation of energy scales: blocking of density/charge flctuations at scale U, then formation of singlet controlled by much smaller scale J_K. For energies much below U but of order J_K, low-energy *effective hamiltonian* in the $N = 2$ sector:

$$H_{\rm eff} \;=\; J_K\, \vec{S}_d \cdot \vec{S}_c \tag{2.20}$$

Physical interpretation: screening out of the impurity spin by the conduction electron bath, through the formation of a singlet ground-state.

All this can be generalized (Schrieffer-Wolf canonical transformation) to a full conduction-electron band, yielding in the same regime an effective hamiltonian (placing the impurity at site 0):

$$H_{\rm K} \;=\; \sum_{\mathbf{k}\sigma} \varepsilon_{\mathbf{k}}\, c^\dagger_{\mathbf{k}\sigma} c_{\mathbf{k}\sigma} \;+\; J_K\, \vec{S}_d \cdot \vec{S}_c(0) \tag{2.21}$$

This is the famous Kondo hamiltonian. The above analysis corresponds to a strong coupling treatment of this hamiltonian for $J_K \gg W$ (W: conduction electron bandwidth). A key question is what happens in the (realistic) case of weak coupling $J_K \ll W$.

Similar considerations apply to the 2-site Hubbard model. In the $N = 2$ singlet sector:

$$\begin{pmatrix} U/2 & t\sqrt{2} & 0 \\ t\sqrt{2} & -U/2 & t\sqrt{2} \\ 0 & t\sqrt{2} & U/2 \end{pmatrix} \tag{2.22}$$

$$(\frac{U}{2} - E)\left(E^2 - \frac{U^2}{4} - 4t^2\right) \;=\; 0 \tag{2.23}$$

$$E = \frac{U}{2} \;\;;\;\; E_\pm \;=\; \pm\frac{U}{2}\sqrt{1 + \frac{16t^2}{U^2}} \tag{2.24}$$

Hence, the ground-state is a non-degenerate singlet (basically inter-site). Since $E_- \;\simeq\; -U/2 - 4t^2/U - \cdots$ for $t \ll U$, the lowering of energy as compared to the triplet is:

$$J \;=\; \frac{4t^2}{U} \tag{2.25}$$

and the effective hamiltonian reads:

$$H_{\rm eff} \;=\; J\, \vec{S}_1 \cdot \vec{S}_2 \tag{2.26}$$

On a full lattice at half-filling, for $J \ll t \ll U$, this yields the Heisenberg model:

$$H_{\rm eff} \;=\; J \sum_{\langle ij \rangle} \vec{S}_i \cdot \vec{S}_j \tag{2.27}$$

with an *antiferromagnetic* coupling $J > 0$.

2.3 Spectral function and Green's function

2.3.1 The case of a local orbital

2.3.2 Generalisation to fermions on a lattice

Chapter 3

Introduction to the Hubbard model

3.1 The Hubbard model defined

$$H = -\sum_{ij\sigma} t_{ij} d^{\dagger}_{i\sigma} d_{j\sigma} + U \sum_{i} \hat{n}_{i\uparrow} \hat{n}_{i\downarrow} \tag{3.1}$$

Chapter 4

From free fermions to Fermi liquids

This section is based on graduate courses given in Geneva (together with C. Berthod, A. Iucci, P. Chudzinski) and in Paris (together with O.Parcollet). For more details, see the course notes: `http://dpmc.unige.ch/gr_giamarchi/` and: `http://www.cpht.polytechnique.fr/cpht/correl/teaching/teaching.htm`

4.1 Non-interacting fermions

Let us start by recalling some well-known but important facts about non-interacting fermion systems. We shall state these facts without detailing the calculations, since they can be found in every textbook on solid-state physics [**?**, **?**].

We consider independent electrons described by the Hamiltonian

$$H_{\rm kin} = \sum_{\vec{k}\nu\sigma} \varepsilon_{\vec{k}\nu} c^\dagger_{\vec{k}\nu\sigma} c_{\vec{k}\nu\sigma} \tag{4.1}$$

When considering fermions in a lattice, the sum over $\vec{k}$ runs over the first Brillouin zone, and ν is a band index (that we shall sometimes omit when focusing on a single band). It is important to keep in mind that the creation/destruction operators in this expression refer to *single-particle wave-functions*. In a lattice, those wave-functions are of the form (Bloch's theorem): $\phi_{\vec{k}\nu}(\vec{r}) = u_{\vec{k}\nu}(\vec{r}) e^{i\vec{k}\cdot\vec{r}}$ with $u_{\vec{k}\nu}$ a Bloch function having the periodicity of the lattice, while in the continuum $\phi_{\vec{k}} = e^{i\vec{k}\cdot\vec{r}}/\sqrt{\Omega}$. The fermion-creation field operator at point $\vec{r}$ is expanded onto these wave-functions as $\psi^\dagger_\sigma(\vec{r}) = \sum_{\vec{k}\nu} \phi^*_{\vec{k}\nu}(\vec{r}) c^\dagger_{\vec{k}\nu\sigma}$.

The eigenstates of (4.1) are Slater determinants of single-particle wave functions, of the form: $\det\{\phi_{\vec{k}_i\nu_i}(\vec{r}_j)\}$, which can conveniently be represented in occupation number basis (Fock representation) as $|\{n_{\vec{k}\nu\sigma}\}\rangle$ with $n_{\vec{k}\nu\sigma} = 0, 1$ when the single-particle state is empty or occupied, respectively. The ground-state for N fermions corresponds to filling all single-particle states with those fermions, starting from the lowest possible single-particle energy and placing two fermions with opposite spin per state. Hence, the ground-state is the 'Fermi-sea':

$$|\mathrm{FS}\rangle = \prod_{\vec{k}\nu,\varepsilon_{\vec{k}\nu}<\varepsilon_F} c^\dagger_{\vec{k}\nu\uparrow} c^\dagger_{\vec{k}\nu\downarrow} |\emptyset\rangle \tag{4.2}$$

In this expression, ε_F is the *Fermi energy*: the largest single-particle energy corresponding to an occupied state. It is also the zero-temperature limit of the chemical potential (assuming a metallic, or liquid, state): $\mu(T \to 0) = \varepsilon_F$. One often incorporates the chemical potential in the energy and define $\xi^0_{\vec{k}\nu} = \varepsilon_{\vec{k}\nu} - \mu$.

In momentum-space, the condition $\varepsilon_{\vec{k}\nu} = \varepsilon_F$ ($\xi^0_{\vec{k}\nu} = 0$) defines the *Fermi surface*. It has important physical significance, since it defines the loci in momentum-space of *zero-energy excitations*. Hence, the presence of a Fermi-surface (FS) is a distinctive aspect of a metallic (or liquid) state, in which excitations with arbitrarily low energy are present, in contrast to an insulating state, in which the ground-state is separated from excited states by an energy gap.

In the context of cold fermionic atoms in optical lattices, a direct imaging of the Fermi surface is possible, as first demonstrated in a remarkable experiment by M. Köhl and coworkers [**?**] for a two-dimensional lattice. The idea is to switch-off the lattice potential adiabatically, so that the quasi-momentum of a fermion in a given quasi-momentum state in the lattice is transferred to the corresponding momentum in the continuum (i.e quasimomentum is conserved to a good approximation) (Fig. 4.1). A time-of-flight expansion and absorption imaging are performed in order to obtain the starting quasi-momentum distribution of the atoms inside the lattice (Fig. 4.2). By changing the lattice depth, a gradual increase of the size of the FS was observed, resulting at some point into a transition from a metal to a band-insulator when the FS coincides exactly with the first Brillouin zone of the lattice. Note that this effect is a consequence of the presence of a confining potential. Indeed, in a homogeneous system, the FS is entirely determined by the number of particles present in the system, and for a given N will remain unchanged if the depth of the lattice (hopping amplitude t) is varied. In contrast, in the presence of a harmonic potential of frequency ω_0,

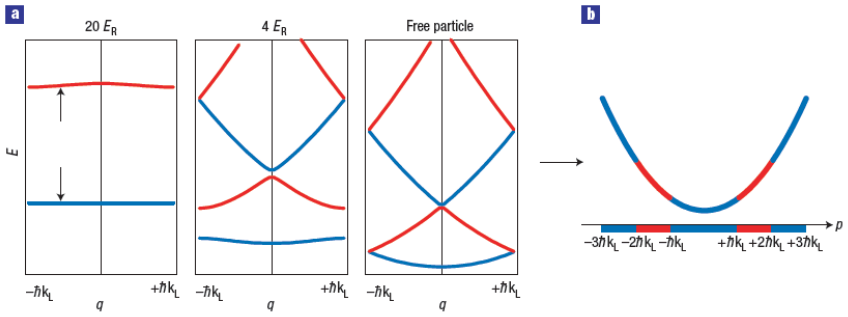

Figure 4.1: "Unfolding" the bandstructure, from a deep lattice to continuum space, while conserving quasi-momentum. Fig. adapted from [**?**]

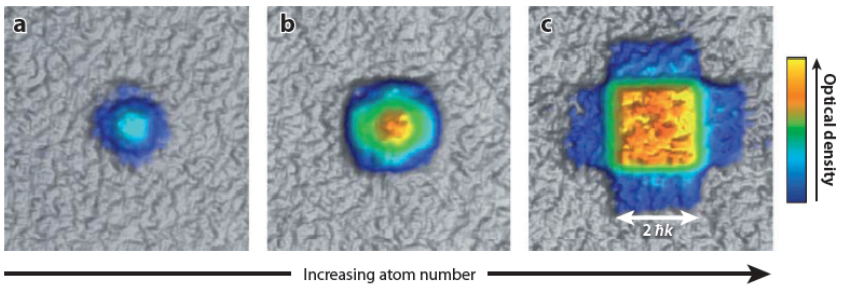

Figure 4.2: Three Fermi-surface images corresponding to low (a), intermediate (b) and higher (c) density of particles per site. In the latter case, the FS extends beyond the first (square) Brillouin zone. From [**?**] and [**?**].

the effective density is $\rho = N(a/l)^3$ with $l = \sqrt{t/m\omega_0^3}$ (see below), and ρ can be changed by changing t.

It is important, at this stage, to have in mind the order of magnitude of key physical parameters (such as density and mass of particles) relevant to different physical systems of interest, namely: liquid Helium 3 (for which Landau Fermi-liquid theory was first developed historically), electrons in solids, and cold atomic gases. Those are summarized in Table 4.1. This table illustrates the fact that the study of degenerate quantum Fermi gases can be undertaken in physical systems with widely different values of the key energy scale: the Fermi energy. While the Fermi temperature ($= \varepsilon_F/k_B$) is a few degrees Kelvin in ^{3}He, it is several tens of thousands of Kelvin for electrons in solids (ε_F is a few eV's) and in the range of a micro- to a nano-Kelvin for cold atomic gases in optical lattices ! The natural unit in

	Mass	Lattice spacing	Density	$T_F = \varepsilon_F/k_B$
Liquid ^{3}He	5.10^{-27}kg		$\sim 2.\,10^{22}$ cm^{-3}	A few K
Electrons in solids	$9.1\,10^{-31}$kg	A few $\mathring{A} \sim 10^{-10}$m	$10^{21} - 10^{23}$cm^{-3}	A few$\times 10^4$K
Cold atoms	m$(^{40}K) \sim 66\,10^{-27}$kg	$\sim \mu$m	$\sim 10^{11} - 10^{12}$cm^{-3}	$\sim$ nK $- \mu$K

Table 4.1: Typical values of physical parameters for three physical systems. Note that, in the absence of a lattice, $\varepsilon_F \propto n^{2/3}/m$.

the latter case is the recoil energy of the atoms in the lattice laser beams $\hbar^2 k_L^2/2m$, typically of order a μK. By those standards it is considerably more difficult to reach the low-temperature (quantum degenerate) regime $T \ll T_F$ for "ultra-cold" atomic gases than for electrons in solids, for which T/T_F is always of order 10^{-2} or less in usual conditions ! This remark can also be turned into an advantage: while the high-temperature crossover between a quantum degenerate and a classical gas cannot be observed easily in solids, it is easily observed with atomic gases. The theoretical description of this crossover (and of the 'incoherent' regime $T \gtrsim T_F$ requires to handle not only very low-energy excitations but also higher-energy excited states, which as explained below, are outside the scope of low-energy effective theories such as Landau Fermi-liquid theory.

At finite temperature, single-particle states of a non-interacting Fermi gas are occupied with a probability given by the Fermi factor (Fig. 4.3):

$$f(\xi^0_{\vec{k}}) = \langle \mathrm{FS}|c^\dagger_{\vec{k}} c_{\vec{k}}|\mathrm{FS}\rangle = \frac{1}{e^{\beta\xi^0_{\vec{k}}}+1} \tag{4.3}$$

In the quantum degenerate regime $T \ll T_F$, the broadening of the Fermi distribution is extremely small. The important states are thus the ones in which particles are excited in a tiny shell close to the Fermi level, as shown in Fig. 4.3. The other excitations are completely blocked by the Pauli principle. This strong constraint on available excited states is of course what confers to fermionic systems their unique properties, and make them so different from a classical system, or from a bosonic quantum system. As a consequence, the specific heat $C = dU/dT = TdS/dT$ is linear with temperature (contrarily to the case of a classical gas for which it would be a constant)

$$C(T) \propto k_{\mathrm{B}}^2 \mathcal{N}(\varepsilon_F) T \ , \ (T \ll T_F) \tag{4.4}$$

where $\mathcal{N}(\varepsilon_F)$ is the density of states at the Fermi level. The compressibility of the fermion gas:

$$\kappa \propto \frac{\partial n}{\partial \mu} \propto \mathcal{N}(\varepsilon_F) \ , \ (T \ll T_F) \tag{4.5}$$

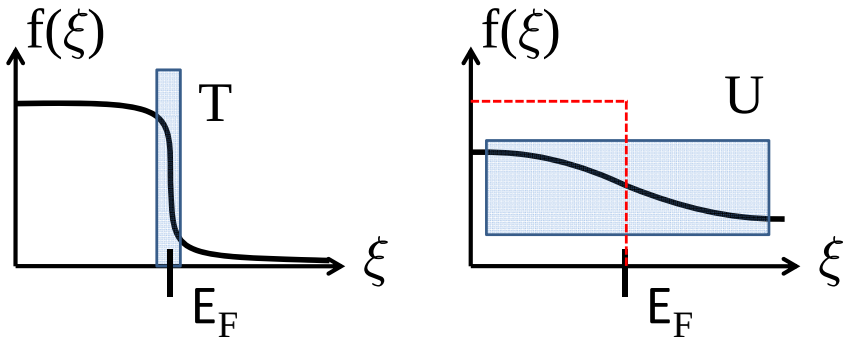

Figure 4.3: Broadening of the Fermi distribution due to the temperature T. Left: when $T \ll T_F$, only a tiny fraction of particles close to the Fermi level can be excited. These low-energy particle-hole excitations control all the physical properties of the system. Right: in the regime $T \gg T_F$, the Fermi factor is broad and high-energy excitations become relevant.

reaches a constant value in the limit $T \to 0$ (in contrast to a band insulator for which ε_F lies within a gap and is hence incompressible $\kappa \propto \mathcal{N}(\varepsilon_F) = 0$). Similarly, the spin susceptibility which measures the magnetization M of the electron gas in response to an applied magnetic field H, reaches a constant value (Pauli behaviour):

$$\chi = \left(\frac{\partial M}{\partial H}\right)_T \propto \mathcal{N}(\varepsilon_F) \ , \ (T \ll T_F) \tag{4.6}$$

Note that a system made of independent spins would have instead a divergent spin susceptibility $\chi \propto 1/T$ when $T \to 0$ (Curie behaviour) instead of a constant one. In a non-interacting Fermi gas, the slope of the specific heat, the compressibility and the spin susceptibility are all controlled by the same quantity, namely the density of states at the Fermi level.

4.2 Quasiparticles and the $(N\pm1)$-particle problem

We now consider the effect of interactions between fermions. We focus on a system which is in a compressible liquid (or metallic) state, with no symmetry breaking of any sort (apart from the translational symmetry breaking due to the lattice). Possible transitions into a (Mott) insulating state induced by interactions, as well as magnetic ordering, will be discussed in

Sec. 5.

The first important observation is that the ground-state wave-function, which was simple in the absence of interactions (the Fermi sea), now becomes exceedingly complex. There are very few cases in which this ground-state wave-function can be found exactly (one such example is the one-dimensional Hubbard model, thanks to Bethe ansatz). Even numerically, the problem is very difficult. The size of the Hilbert space grows exponentially with the size of the system (for example, for a single-band Hubbard model, it has dimension 4^{N_s} with N_s the number of lattice sites). Hence, exact diagonalization (e.g. Lanczos) methods can only handle small systems (say, $N_s \lesssim 12$). As to quantum Monte-Carlo simulations, they are faced with the infamous 'minus-sign problem' which severely limit their use, at least when doing direct simulations without further approximations.

The second important observation is that we may not care so much, after all, about the detailed form of the ground-state wave-function. What most experiments actually probe are the *excitations* above the ground-state[**?**]. Furthermore, if the system is at low temperature ($T \ll T_F$) and probed in a gentle-enough manner, only low-energy excitations matter. So what we really want is a description of these low-energy excitations. This is fortunate, since general wisdom (backed up by renormalization-group ideas) teaches us that low-energy phenomena (or, equivalently, phenomena involving long time scales) have a large degree of *universality*. Hence, the nature of the low-energy excitations may not depend on all the microscopic details of the specific problem at hand, and a universal effective theory of those low-energy excitations may be in sight. For interacting fermions in more than one dimension, this universal theory is Landau's Fermi-liquid theory[**?**, **?**]. For one-dimensional systems, it is Luttinger liquid theory (Secs. **??**,**??**).

A word of warning, however: being effective theories of low-energy excitations, their applicability is limited to... low-energy. Hence, these descriptions come with a characteristic scale above which they are no longer valid and a more detailed quantitative description is required. This scale is associated, as we shall see, with the lifetime of quasiparticles: for energies above a certain coherence scale, long-lived quasiparticles no longer make sense and Landau Fermi liquid theory does not apply. In strongly correlated systems, this coherence scale may be quite low, making the range of validity of effective theories too limited to explain all experimental observations. Also, experiments that perturb the system too strongly (e.g. in a pump-probe experiment) require tools beyond low-energy effective theories.

4.2.1 Quasiparticles: qualitative picture

The basic idea behing Landau Fermi liquid theory is that the low-energy excited states can be constructed by combining together elementary excitations, with combination rules and quantum numbers identical to that of free particles.

For free fermions, this is clearly the case: the simplest low-energy excitation (at constant particle number N) is obtained by considering a single Slater determinant which is obtained from the Fermi sea by exciting an electron from a state just below the FS to a state just above. Hence, a 'particle-hole' excitation has been created, which is a combination of a hole-like excitation (removing a particle) and a particle-like excitation (adding a particle). In a free system, adding a particle in an empty state yields an eigenstate: such an excitation does not care about the presence of all the other electrons in the ground state (otherwise than via the Pauli principle which prevents from creating it in an already occupied state).

In the presence of interactions this will not be the case and the added particle interacts with the existing particles in the ground state. For example for repulsive interactions one can expect that this excitation repels other electrons in its vicinity. This is schematically represented in Fig. 4.4. On the other hand if one is at low temperature (compared to the Fermi energy) there are very few such excitations and one can thus neglect their mutual interactions (or rather treat them in a mean-field manner). This defines a new composite object (fermion or hole surrounded by its own polarization cloud). This complex object essentially behaves as a particle, with the same quantum numbers (charge, spin) than the original fermion, albeit with renormalized parameters, for example its mass. This image thus strongly suggests that even in the presence of interactions good elementary excitations looking like free particles, still exists. These particle resemble free fermions but with a renormalized excitation energy $\xi_{\vec{k}}$, different from $\xi^0_{\vec{k}}$.

Since our system is gapless, the excitation energy $\xi_{\vec{k}}$ must vanish on a certain surface in momentum-space. This defines the Fermi surface *of the interacting system*. Note that, in contrast to the free system, we have established no connection between the FS and the ground-state wave-function: we have been referring only to excitation energies. Under quite general assumptions, a remarkable property does hold however (even when quasiparticles do not exist in the Landau sense) : the momentum-space volume encompassed by the FS is identical to that of the free system (*Luttinger theorem*), and hence entirely fixed by the number of particles. The *shape of the FS*, however, can be changed by interactions (except in the continuum, where it

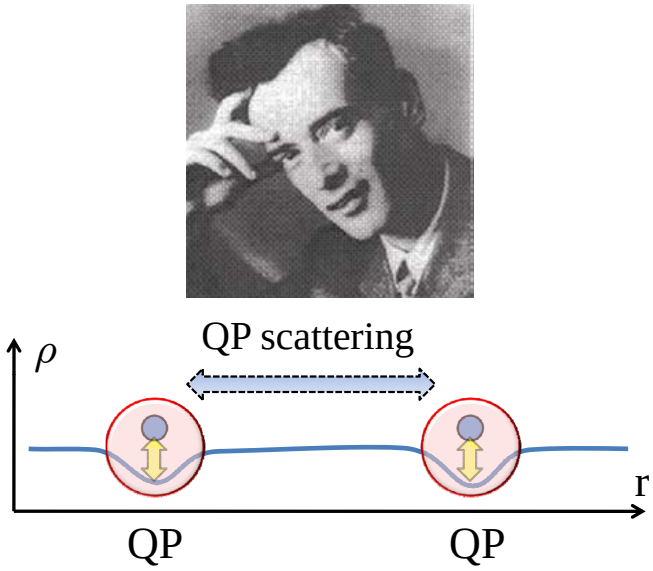

Figure 4.4: Top: Lev Landau, the man behind the Fermi liquid theory (and many other things). Bottom: In a Fermi liquid, the few excitations above the ground state can interact strongly with all the other electrons present in the ground state. The effect of such interactions is strong and lead to a strong change of the parameters entering the low-energy effective theory, compared to free electrons. The combined object behaves as a long-lived particle, named a quasiparticle: its characteristics depend strongly on interactions. However the scattering of the quasiparticles is blocked by the Pauli principle leaving a very small phase space for scattering. The lifetime of the quasiparticles is thus extremely large. Furthermore, a low-energy excited state involves a low-density of excited quasiparticles. This is the essence of the Fermi liquid theory.

is a sphere specified only by its radius k_F given by $2 \times \frac{4}{3}\pi k_F^3/h^3 = \frac{N}{\Omega}$).

The dispersion relation $\xi_{\vec{k}}$ specifying the quasiparticles excitation energy can be expanded around a given point $\vec{k}_F$ of the FS as:

$$\xi_{\vec{k}} = \nabla_{\vec{k}}\xi|_{\vec{k}_F} \cdot (\vec{k} - \vec{k}_F) + \cdots \tag{4.7}$$

which defines a renormalized Fermi velocity of the quasiparticles at this point: $\vec{v}^*(\vec{k}_F) = \nabla_{\vec{k}}\xi|_{\vec{k}_F}/\hbar$. In the continuum, the Fermi velocity is identical on all points of the spherical FS (by isotropy) and it is customary to define the *effective mass* of quasiparticles by analogy to the free-particle dispersion relation $\xi^0_{\vec{k}} = \hbar^2k^2/2m - \hbar^2k_F^2/2m \sim \hbar k_F(k - k_F)/m + \cdots$:

$$\xi_{\vec{k}} = \frac{\hbar k_F}{m^*}(k - k_F) + \cdots \tag{4.8}$$

The effective mass controls the low-temperature behaviour of the specific heat of a Landau Fermi-liquid, which has the same linear-temperature dependence than a free fermion gas:

$$\frac{(C/T)}{(C/T)_0} = \frac{\mathcal{N}_{\rm QP}}{\mathcal{N}}|_{\rm FS} = \frac{m^*}{m} \tag{4.9}$$

While the low-temperature compressibility and susceptibility are again constant:

$$\frac{\kappa}{\kappa_0} = \frac{m^*/m}{1 + F_0^s} \ , \ \frac{\chi}{\chi_0} = \frac{m^*/m}{1 + F_0^a} \tag{4.10}$$

but involve distinct renormalizations, which parametrize the effective interaction between quasiparticles in the low-energy effective theory (Landau parameters F_0^s and F_0^a). Note that expressions (4.9,4.10) have been written for the isotropic case (continuum). In a anisotropic lattice case, the Landau parameters acquire a more complex angular dependence and these expressions have less predictive power.

4.2.2 The $N \pm 1$-particle problem: Green's function, spectral function and self-energy

Of course, the above are qualitative ideas. Let us now turn to a more formal treatment. To this aim, we imagine probing the excitations of the N-particle system by removing a fermion from the system (at, say, point $\vec{r}$ and time 0) and sending it to the outside vacuum, or by injecting a fermion from the outside (Fig. 4.5). Starting from the (complicated) ground-state $|\Psi_0\rangle$ of the N-particle system, we thus prepare the wave-function (for simplicity, we

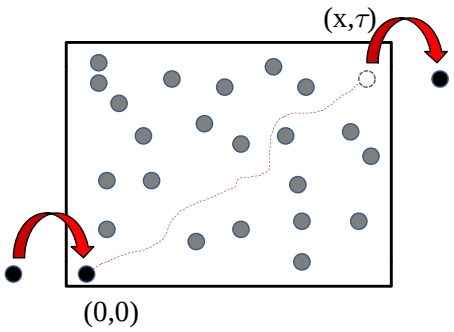

Figure 4.5: A *gedanken* experiment probing the excitations of an interacting system. A particle is injected from outside at point $\vec{r}$ and time $t = 0$. It propagates through the system and partially decays by creating excitations. The particle is removed at position $\vec{r'}$ and time t. The amplitude of this process contains a wealth of information about single-particle excitations of the system, encapsulated in the spectral function $A(\vec{k}, \omega)$. "Resemblance" of the final state with the original bare particle signals the existence of long-lived quasiparticle excitations.

consider a one-band system and one spin component, so that we omit both indices ν, σ):

$$|\Psi(\vec{r}, 0)\rangle \equiv \psi^\dagger(\vec{r}, t)|\Psi_0\rangle = \sum_{\vec{k}} \phi^*_{\vec{k}}(\vec{r})\, c^\dagger_{\vec{k}}|\Psi_0\rangle \tag{4.11}$$

In a non-interacting system, the wave functions on the right-hand side are eigenstates of the system with $N + 1$ particles. But this is not the case in the presence of interactions. Hence, in order to understand the time-evolution of this wave-function, we expand it onto the *exact eigenstates* of the $N + 1$-particle system:

$$|\Psi(\vec{r}, 0)\rangle = \sum_{\vec{k}} \phi^*_{\vec{k}}(\vec{r}) \sum_A \langle\Psi_A|c^\dagger_{\vec{k}}|\Psi_0\rangle|\Psi_A\rangle \tag{4.12}$$

We then time-evolve this state with the evolution operator $\exp -\frac{i}{\hbar}(\hat{H} - \mu\hat{N})$, with $\hat{H}$ the full (interacting) many-body hamiltonian, yielding the state $|\Psi(\vec{r}, t)\rangle$. We compare this state with the state obtained by injecting a fermion into the ground-state directly at time t, and point $\vec{r'}$, $\psi^\dagger(\vec{r'})|\Psi_0(t)\rangle$, by forming the overlap of the two states $\langle\Psi_0(t)\psi(\vec{r'})|\Psi(\vec{r}, t)\rangle$. This overlap

can also be viewed as the amplitude for injecting a particle at $\vec{r}$ at time 0 and removing it at $\vec{r'}$ at time t (Fig. 4.5). It reads:

$$\langle\Psi_0|\psi(\vec{r'},t)\psi^\dagger(\vec{r},0)|\Psi_0\rangle = \sum_{\vec{k}} \phi_{\vec{k}}(\vec{r'})\phi^*_{\vec{k}}(\vec{r}) \sum_A |\langle\Psi_A|c^\dagger_{\vec{k}}|\Psi_0\rangle|^2 \, e^{-\frac{i}{\hbar}[E_A-(E_0+\mu)]t} \tag{4.13}$$

Note that $\mu = \partial E_0/\partial N$ and thus the ground-state energy of the $N+1$-particle system is (for a large gapless system) $E_0^{N+1} \simeq E_0 + \mu$. Hence, the frequencies appearing in the time-evolution on the r.h.s involve the excitation energies $\hbar\omega = E_A - E_0^{N+1} > 0$ of the $N+1$-particle system. We see that this *gedanken* experiment provides information on the excitation of the system, more precisely on the excited states to which $|\Psi_0\rangle$ couples by injecting a particle. It is very useful to introduce the *one-particle spectral function*, which condenses all this information, and is defined (at $T=0$) as:

$$\begin{aligned} A(\vec{k},\omega) &\equiv \sum_{A(N+1)} |\langle\Psi_A|c^\dagger_{\vec{k}}|\Psi_0\rangle|^2 \, \delta\left[\omega - \frac{1}{\hbar}(E_A - E_0 - \mu)\right] \quad , \quad (\omega > 0) \\ &\equiv \sum_{B(N-1)} |\langle\Psi_B|c_{\vec{k}}|\Psi_0\rangle|^2 \, \delta\left[\omega - \frac{1}{\hbar}(E_0 - \mu - E_B)\right] \quad , \quad (\omega < 0) \end{aligned} \tag{4.14}$$

It is easily checked that the spectral function is normalized over frequencies for each value of the momentum: $\int_{-\infty}^{+\infty} A(\vec{k},\omega)d\omega = 1$ and that the quasi-momentum distribution of particles in the ground-state is given by: $N(\vec{k}) \equiv \langle\Psi_0|c^\dagger_{\vec{k}}c_{\vec{k}}|\Psi_0\rangle = \int_{-\infty}^{0} A(\vec{k},\omega)d\omega$. The spectral function can also be related to the Fourier transform of the *retarded Green's function*, defined as:

$$G(\vec{k},t) = -i\,\theta(t)\langle\Psi_0|[c_{\vec{k}}(t), c^\dagger_{\vec{k}}(0)]_+|\Psi_0\rangle \tag{4.15}$$

by:

$$A(\vec{k},\omega) = -\frac{1}{\pi}\,\mathrm{Im}G(\vec{k},\omega) \tag{4.16}$$

In Fig. 4.6, we display a cartoon of the spectral function of a Fermi liquid. For momenta not too far from the Fermi surface, it can be decomposed into two spectral features: a narrow peak corresponding to quasiparticle excitations, and a broad continuum corresponding to incoherent excitations. The narrow peak is centered at the excitation frequency $\omega = E_{\vec{k}} - \mu = \xi_{\vec{k}}$ corresponding to the quasiparticle dispersion. It has a spectral weight $Z_{\vec{k}} \leq 1$ and its width $\gamma_{\vec{k}} = \hbar/\tau_{\vec{k}}$ corresponds to the inverse lifetime of quasiparticle excitations and can be approcimated by a Lorentzian:

$$A_{\mathrm{QP}}(\vec{k},\omega) \simeq Z_{\vec{k}} \, \frac{\gamma_{\vec{k}}/\pi}{(\omega - \xi_{\vec{k}})^2 + \gamma^2_{\vec{k}}} \tag{4.17}$$

Correspondingly, the Green's functions can be separated into two components, involving very different time-scales:

$$G(\vec{k},\omega) \simeq Z_{\vec{k}}\, e^{-t/\tau_{\vec{k}}}\, e^{-i\xi_{\vec{k}}\, t/\hbar} \,+\, G_{\rm inc}(\vec{k},t) \tag{4.18}$$

The notion of quasiparticle excitations makes sense because their lifetime $\tau_{\vec{k}}$ becomes very large as $\vec{k}$ approaches the Fermi surface, for phase-space reasons detailed in the next section. As a result, the first term decays very slowly, while the second "incoherent" one decays fast (corresponding to a broad frequency spectrum).

A very useful quantity is the *self-energy*, which is a measure of the difference between the Green's function of the interacting system and that of the free system. It is defined by (with $\xi^0_{\vec{k}} = \varepsilon_{\vec{k}} - \mu$):

$$G(\vec{k},\omega) = \frac{1}{\omega - \xi^0_{\vec{k}} - \Sigma(\vec{k},\omega)} \tag{4.19}$$

By expanding this expression close to the FS $\vec{k} \simeq \vec{k}_F$ and at low-frequency $\omega \simeq 0$, we find that the key quantities characterizing quasiparticles can be read-off from the self-energy. The FS of the interacting system are formed by the quasi-momenta which satisfy:

$$\varepsilon_{\vec{k}_F} \,+\, \Sigma(\vec{k}_{\rm F},0) \,=\, \mu \tag{4.20}$$

in which μ in the r.h.s should be viewed as a function of the particle density n, and of course of the interaction strength. The quasiparticle spectral weight, dispersion $\xi_{\vec{k}} = \vec{v}^*(\vec{k}_{\rm F})\cdot(\vec{k}-\vec{k}_{\rm F})$, and inverse lifetime are given by:

$$\begin{aligned} Z_{\vec{k}} &= \left[1 - \frac{\partial \Sigma'}{\partial \omega}|_{\omega=0}\right]^{-1} \\ \vec{v}^*(\vec{k}_{\rm F}) &= Z_{\vec{k}_{\rm F}} \left[\nabla_{\vec{k}}\xi^0_{\vec{k}} + \nabla_{\vec{k}}\Sigma'\right]_{\omega=0,\vec{k}=\vec{k}_{\rm F}} \\ \gamma_{\vec{k}} &= Z_{\vec{k}}\, \Sigma''(\vec{k},\omega=\xi_{\vec{k}}) \end{aligned} \tag{4.21}$$

In these expressions, Σ' and Σ'' stand for the real and imaginary parts of the retarded self-energy, respectively. As expected, the inverse quasiparticle lifetime is related to the latter (but also involves the weight Z, which in contrast would not appear in the scattering rate measured from transport or optical conductivity). For an isotropic system this leads to the following expression for the effective mass:

$$\frac{m}{m^*} \,=\, Z\, \left[1 + \frac{m}{\hbar k_F}\frac{\partial \Sigma'}{\partial k}|_{\omega=0,k=k_F}\right] \tag{4.22}$$

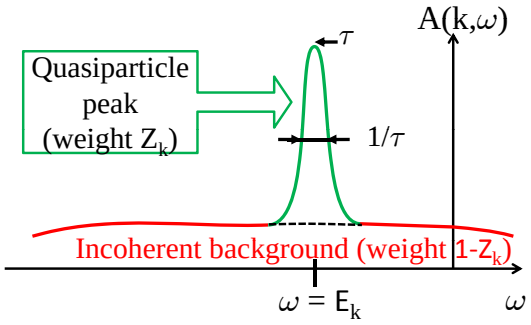

Figure 4.6: A cartoon of the spectral function for interacting particles. One can recognize several features. There is a continuous background of excitations of total weight $1 - Z_{\vec{k}}$. This part of the spectrum corresponds to incoherent excitations which are not associated with quasiparticles. In addition to this continuous background, there is a quasiparticle peak. The total weight of the peak $Z_{\vec{k}}$ is determined by the real part of the self energy. The center of the peak is at a frequency $\xi_{\vec{k}}$, the renormalized quasiparticle dispersion. The quasiparticle peak has a lorentzian lineshape that reflects the finite lifetime of the quasiparticles, inversely proportional to the imaginary part of the self energy.

Note that the quasiparticle weight is related only to the frequency-dependence of the self-energy, while the effective mass involves both the frequency and momentum dependence. Only when the self-energy is momentum-independent (as e.g. in the limit of large dimensionality, or within the dynamical mean-field theory approximation) do we have $m^*/m = 1/Z$.

On general grounds, the following phenomena are clear signatures of strong correlations (and need not necessarily occur together):

- A small quasiparticle weight Z
- A large effective mass (low $\vec{v}^*_F$)
- A short quasiparticle lifetime (large $\gamma_{\vec{k}}$).

4.2.3 Lifetime of quasiparticles:phase-space constraints

In order to estimate the lifetime of a quasiparticle let us look at the scattering of a particle from a state $\vec{k}$ to another state. Let us start from the non

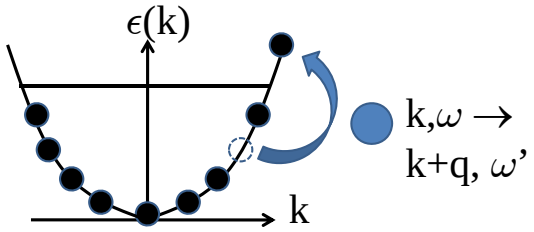

Figure 4.7: Cartoon of the process giving the lifetime of a particle with energy ω. The ground-state of the free system has all single-particle states filled below the Fermi energy ε_F. The excitations are thus particle-hole excitations where a particle is promoted from below the Fermi level to above the Fermi level. Due to the presence of the sharp Fermi level, the phase space available for making such a particle-hole excitations is severely restricted.

interacting ground state in the spirit of a perturbative calculation in the interactions. As shown in Fig. 4.7 a particle coming in the system with an energy ω and a momentum $\vec{k}$ can excite a particle-hole excitation, taking a particle below the Fermi surface with an energy ω_1 and putting it above the Fermi level with an energy ω_2. The process is possible if the initial state is occupied and the final state is empty. One can estimate the probability of transition using the Fermi golden-rule. The probability of the transition gives directly the inverse lifetime of the particle, and thus the imaginary part of the self energy. We will not care here about the matrix elements of the transition, assuming that all possible transitions will effectively happen with some matrix element. The probability of transition is thus the sum over all possible initial states and final states that respect the constraints (energy conservation and initial state occupied, final state empty). Since the external particle has an energy ω it can give at most ω in the transition. Thus $\omega_2 - \omega_1 \leq \omega$. This implies also directly that the initial state cannot go deeper below the Fermi level than ω otherwise the final state would also be below the Fermi level and the transition would be forbidden. The probability of transition is thus

$$P \propto \int_{-\omega}^{0} d\omega_1 \int_{0}^{\omega+\omega_1} d\omega_2 = \frac{1}{2}\omega^2 \tag{4.23}$$

One has thus the remarkable result that because of the *discontinuity* due to the Fermi surface and the Pauli principle that only allows the transitions

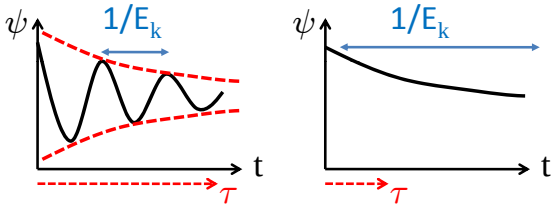

Figure 4.8: For particles with an energy E_k and a finite lifetime τ, the energy controls the oscillations in time of the wavefunction. (Left:) In order to properly identify an excitation as a particle it is mandatory that the wavefunction oscillates several time before being damped by the lifetime. (Right:) In contrast, if the damping is too fast, it is impossible to define precisely the frequency of the oscillations, and thus a precise excitation energy associated with a long-lived quasiparticle.

from below to above the Fermi surface, the inverse lifetime behaves as ω^2. This has drastic consequences since it means that contrarily to the naive expectations, when one considers a quasiparticle at the energy ω, the lifetime grows much *faster* than the period $\tau_\omega = 2\pi/\omega$ characterizing the oscillations of the wavefunction (Fig. 4.8). In fact

$$\frac{\tau_{\rm QP}}{\tau_\omega} \propto \frac{1}{\omega} \to \infty \tag{4.24}$$

when one approaches the Fermi level. In other words the Landau quasiparticles become *better and better defined* as one gets closer to the Fermi level. This is a remarkable result since it confirms that we can view the system as composed of single particle excitations that resemble the original electrons, but with renormalized parameters (effective mass m^*, quasiparticle weight Z_k, etc.).

4.2.4 Probing quasiparticles: photoemission and outcoupling spectroscopies

Experimental spectroscopic techniques are available, which to a good approximation realize in practice the *gedanken* experiment of Fig. 4.5, and hence allow for a direct imaging of quasiparticle excitations.

In the solid-state context, angular-resolved photoemission spectroscopy (ARPES) is a remarkable experimental method which has undergone considerable development over the past two decades (stimulated to a large extent

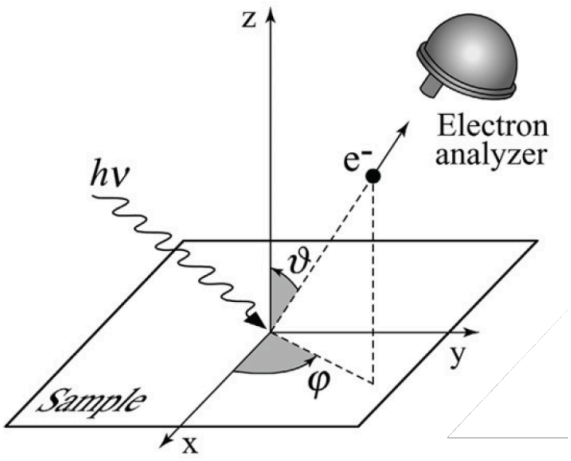

Figure 4.9: Basic principle of photoemission spectroscopy. A photon beam is sent onto the (carefully cleaved) surface of the sample. An electron is extracted (photoelectric effect) and its energy and momentum is recorded from the electron analyzer. (Adapted from [**?**]).

by the study of high-T_c superconductors) see e.g. [**?**, **?**]. The basic principle of this method is illustrated on Fig. 4.9. Under certain conditions and approximations, the measured photoemission intensity is given by:

$$I(\vec{k},\omega) \;=\; M(\vec{k},\omega)\, A(\vec{k},\omega)\, f(\omega) \tag{4.25}$$

In this expression, M is a matrix element, $A(\vec{k},\omega)$ is the one-particle spectral function introduced above, and $f(\omega)$ is the Fermi distribution. In addition, because of the finite energy resolution, the measured signal is a convolution of (4.25) with a Gaussian of a certain width. Currently available energy resolutions depend a lot on the incident photon energy: it is typically of order $50-100$ meV when using X-rays with energies of several hundred eV's at the synchrotron, of order $5-10$ meV for laboratory sources such as a Helium lamp (~ 21 eV), and as low as a fraction of a meV for the recently developed laser-based photoemission ($h\nu \sim 6$ eV). These different sources provide complementary information, since there is a trade-off between bulk vs. surface sensitivity, energy resolution, and the momentum-space constraints limiting the area of the Brillouin zone that can be probed.

The Fermi function appears in expression (4.25) because this spectroscopy measures the probability for extracting an electron from the system, and

hence *mostly probes hole-like excitations*. Momentum-resolved spectroscopies of particle-like excitations have unfortunately a much poorer resolution. Scanning tunneling microscopy (STM), in contrast, does probe both $\omega < 0$ and $\omega > 0$, but in a momentum-integrated way.

As an example, Fig. 4.10 displays ARPES measurements on Sr_2RuO_4, a two-dimensional transition-metal oxide with strong electronic correlations. This material has a three-sheeted FS, which can be beautifully imaged with ARPES (as well as with other techniques, such as quantum oscillations in a magnetic field, with good agreement between these two determinations of the FS). On Fig. 4.10 (right side), the photoemission signal is displayed along a certain cut ($M - \Gamma$) in momentum-space which reveals quasiparticle peaks corresponding to two of these FS sheets. For momenta $\vec{k}$ far from the FS, only a broad incoherent signal is seen. With $\vec{k}$ approaching $\vec{k}_F$, a peak develops revealing the quasiparticles. When $\vec{k}$ crosses the FS into empty states, the signal disappears because of the Fermi factor. Careful examination of these spectra show that the quasiparticle peak becomes more narrow as the FS is approached, as expected from the (Landau) phase-space arguments above.

In the context of cold atomic gases, an analogue of photoemission spectroscopy can also be performed [**?**, **?**], see also [**?**, **?**] and references therein. The idea there is to trigger the conversion of one of the hyperfine state (say, $|1\rangle$) present in the system of interest into an out-coupled state $|3\rangle$. This can be achieved either by exciting the system with radio-frequencies (rf spectroscopy) or by inducing a stimulated Raman transition using two laser beams (Fig. 4.11). A time-of-flight measurement can then be performed which allows for a determination of the initial momentum $\vec{k}$ of the outcoupled atom. When studying for example an interacting mixture of two hyperfine species $|1\rangle, |1'\rangle$, one would ideally like to pick the out-coupled state $|3\rangle$ such that it has only very weak interactions with either $|1\rangle$ or $|1'\rangle$. Under such conditions, the production rate of outcoupled atoms is obtained from Fermi's golden-rule as:

$$\begin{aligned} R_{\vec{q}}(\vec{k},\omega) &= \frac{2\pi}{\hbar}\sum_{\mathbf{r}} W_{\vec{k}}^{\vec{q}}\,|\Omega(\vec{r})|^2\; f(\varepsilon^{\vec{r}}_{3,\vec{k}} - \hbar\omega - \mu_0) \\ &\qquad \times A(\vec{k}-\vec{q}, \varepsilon^{\vec{r}}_{3,\vec{k}} - \mu_0 - \hbar\omega; \mu_{\vec{r}}). \end{aligned} \tag{4.26}$$

In this expression, $\vec{q} = \vec{k}_1 - \vec{k}_2$ is the momentum difference between the two laser beams in a Raman setup (the case of rf-spectroscopy amounts simply to set $\vec{q} = \vec{0}$). $\vec{r}$ denotes a given point in the trap, with $\mu_{\vec{r}} = \mu_0 - V_1(\vec{r})$ the local chemical potential (using the LDA approximation) and μ_0 the

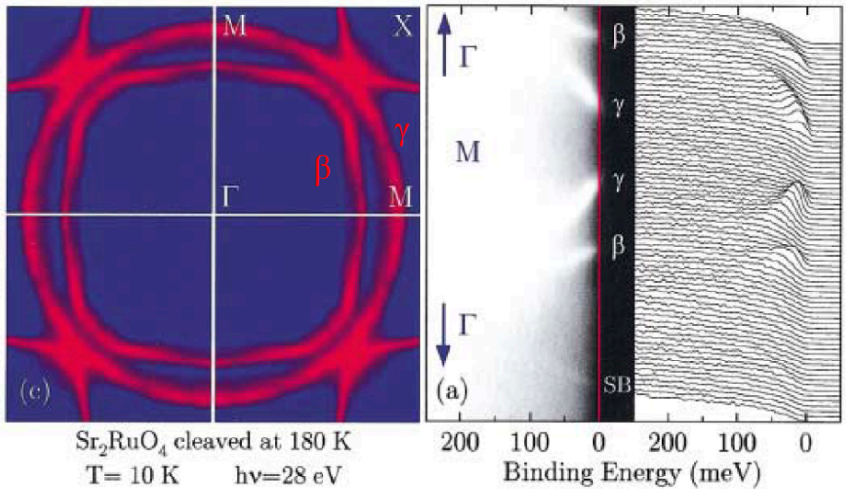

Figure 4.10: ARPES spectroscopy of Sr_2RuO_4. Left: ARPES intensity map providing a determination of the Fermi surface, which has three sheets (α, β, γ). Right: Energy-dependence of the photoemission signal (energy-distribution curves, or EDCs) for several momenta along the Γ-M-Γ direction in the Brillouin zone. Clear quasiparticle peaks are seen when approaching the FS crossing of the β- and γ-sheets. After [**?**].

chemical potential at the center of the trap. $\Omega(\vec{r})$ is the Rabi frequency of the transition and $\omega = \omega_{12} - \omega_{23}$ (Fig. 4.11). $W_{\vec{k}}^{\vec{q}}$ is a matrix element involving Wannier functions in the lattice and $\varepsilon_{3,\vec{k}}^{\vec{r}} = \varepsilon_{3,\vec{k}} + V_3(\vec{r})$ is the dispersion of the outcoupled atom corrected by its trapping potential.

The main message of this expression is that, as in photoemission spectroscopy, measuring the outcoupling rate provides access to the spectral function (provided certain conditions are met). On Fig. 4.11, we display theoretical results for the fermionic Hubbard model in a strongly correlated regime, which demonstrate that the key features seen in the spectral function (quasiparticle peak and incoherent lower Hubbard band) can be detected by rf or Raman outcoupling spectroscopy.

Recently, the JILA group performed a beautiful experiment [**?**] in which the single-particle excitations of a trapped fermionic gas were measured using energy- and momentum- resolved rf-spectroscopy, hence demonstrating the usefulness of such spectroscopic probes. Some of their results are reproduced on Fig. 4.12.

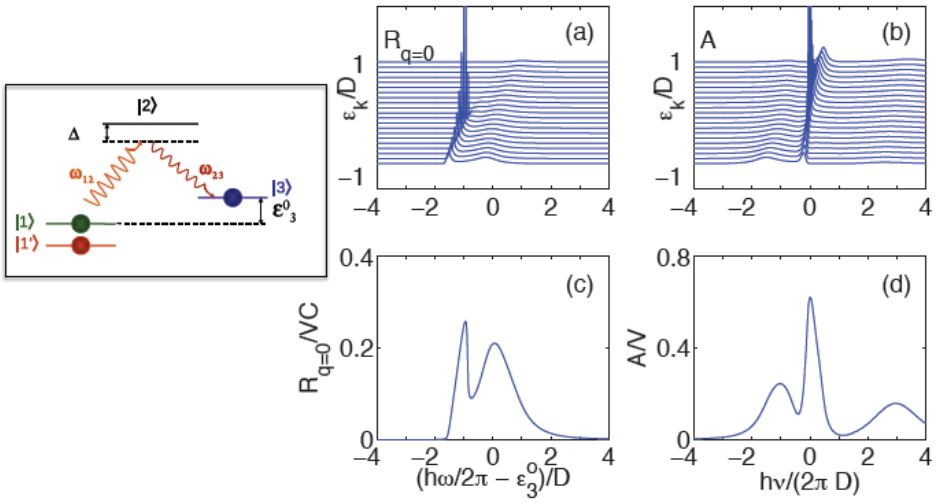

Figure 4.11: Left: Raman outcoupling process. Atoms in hyperfine state $|1\rangle$ are transferred to state $|3\rangle$ using two laser beams with frequencies ω_{12}, ω_{23}. Right: Theoretical spectra for a homogenous Hubbard model in a strongly-correlated regime $U/W = 1.75$ (with W the bandwidth) and total density per site $n = 0.85$, as obtained from dynamical mean-field theory. (a-b): momentum-resolved rf-spectra (a) and spectral function (b). (c-d): momentum integrated rf-spectrum (c) and spectral function (d). Three main features are seen on the spectral function: upper and lower Hubbard bands corresponding to incoherent, high-energy, quasi-local excitations, and a sharp dispersing quasi-particle peak near the Fermi level. Both the quasiparticle peak and lower Hubbard band are seen in the outcoupled spectra. From [**?**].

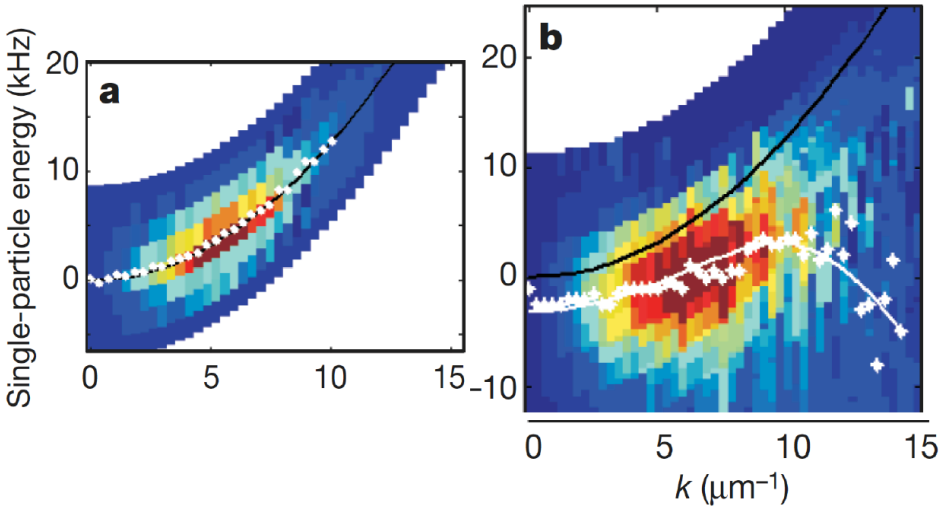

Figure 4.12: "Photoemission" spectroscopy of a two-component trapped gas of ^{40}K fermionic atoms. Displayed are intensity maps obtained by energy- and momentum- resolved rf-spectroscopy. (a): Data for a very weakly interacting gas, showing the expected parabolic dispersion of excitations. (b): Data close to unitarity $1/k_F a \sim 0$. From [**?**].

Chapter 5

Mott transition of fermions: three dimensions

In this section, we consider again the physics of Mott localization, this time in the context of a two-component gas of fermions in an optical lattice with a repulsive interaction. In comparison to the bosonic case considered in Sec.1, a major novelty here is the existence of an internal degree of freedom (the two hyperfine states, or the spin in the case of electrons in a solid). This leads to the possibility of long-range "magnetic" ordering. Even so, it is important to keep in mind that the basic physics behind the Mott localization of fermions is identical to the bosonic case, at least at strong coupling $U \gg t$. Namely, the repulsive interaction makes it unfavorable for particles to hop, resulting in an incompressible state with suppressed density fluctuations.

5.1 Homogeneous system: the half-filled Hubbard model

On Fig. 5.1, we display the phase diagram of the fermionic Hubbard model for a three-dimensional cubic lattice and a homogeneous density of one particle per site on average ("half-filled band"). From the point of view of symmetry breaking and long-range order, there are only two phases. Below the Néel temperature $T_N(U)$ (plain/red line), antiferromagnetic long-range order occurs, in which spin and translational symmetries are broken. At $T = 0$ this phase has a gap and is an insulator. The phase $T > T_N$ is a paramagnet (no long-range spin ordering). However, physically important *crossovers* take place within this phase. The short-dashed line in Fig. 5.1 denotes the

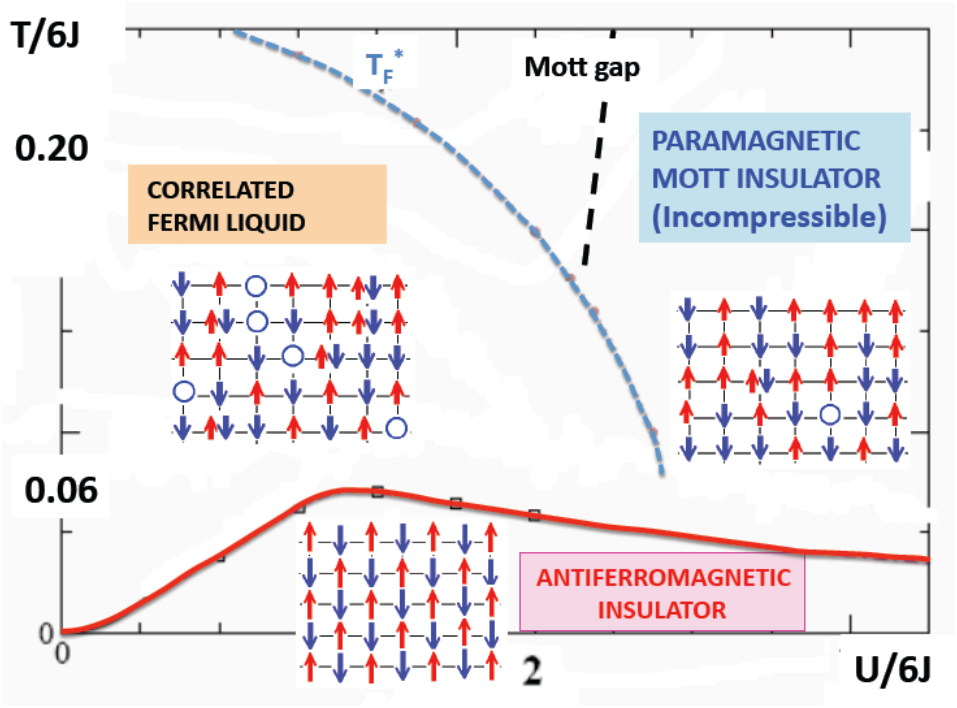

Figure 5.1: Phase diagram of the homogeneous Hubbard model, for a three-dimensional cubic lattice with one-particle per site on average. The plain line (red) denotes the phase transition into a long-range ordered antiferromagnet (Néel temperature). The long-dashed line (black) denotes the Mott gap: to the right of this line the paramagnetic phase behaves as an incompressible Mott insulator. The short-dashed line (blue) denotes the quasiparticle coherence scale. To the right of this line, the paramagnetic phase behaves as an itinerant fermionic liquid with long-lived quasiparticles. Typical snapshots of the wave-function in real space are displayed for each regime.

coherence scale of quasiparticles $T_F^*(U)$. For $T < T_F^*$ (i.e. low-enough temperature and weak-enough coupling) one has an itinerant fermionic liquid, with long-lived quasiparticles (essentially a Fermi liquid, apart from possible subtleties associated with perfect nesting). Another key energy scale is the Mott gap (long-dashed line), which is of order $\Delta_g \sim U$ at large U. For $T < \Delta_g$, one has an essentially incompressible Mott insulator (up to very rare thermal excitations), with frozen density fluctuations and a high spin entropy, i.e. a localized paramagnet.

Hence, when increasing the strength of the repulsive coupling U/t, one crosses over from a fermionic liquid to an incompressible localized paramagnet (through an intermediate incoherent state which is a "bad metal" or a poor insulator). In a situation where magnetic long-range order is suppressed (e.g. due to geometrical frustration of the lattice), this crossover may be replaced by a true phase transition. Because no symmetry breaking distinguishes a metal from an insulator at finite temperature, this transition is expected to be first-order at $T \neq 0$, similar to a liquid-gas transition. The precise description of this crossover or transition is not so easy theoretically. Indeed, in contrast to the phase transition between a superfluid and a Mott insulator of bosons, there is no evident order parameter associated with a static correlation function which discriminates between a metal and a paramagnetic Mott insulator of fermions. Possible order parameters are all related to frequency-dependent (dynamical) response functions: for example the Drude weight associated with the $\omega \to 0$ component of the ac-conductivity, or the quasiparticle weight Z introduced above and associated with the low-frequency behaviour of the one-particle Green's function. For this reason, a mean-field theory of this crossover or transition must focus on one- or two-particle response functions. Currently, the most complete approach of this kind is dynamical mean-field theory (DMFT), which has allowed for many successes in understanding strongly-correlated fermion systems. For brevity, we refer the reader to review articles for a presentation of this theoretical approach.

5.1.1 From Mott to Slater

The transition into the antiferromagnetic state deserves some further remarks. At strong coupling $U/t \gtrsim u^*$, there is a clear separation of energy scales: the gap Δ_g ($\sim U$ at large U) is much larger than the antiferromagnetic superexchange $J_{\rm AF} \sim t^2/U$ which also controls $T_N \propto J_{\rm AF}$. Hence for $T \ll \Delta_g$, density fluctuations are frozen out, particles are localized into a Mott insulating state and only the spin degrees of freedom are active which

are described by an effective Heisenberg model. In this Mott regime, localization precedes spin ordering which is a low-energy instability of the insulating paramagnet. In contrast, at weak coupling $U/t \ll u^*$, long-range magnetic order and the blocking of translational degrees of freedom cannot be distinguished: in this regime the opening of a gap is intimately connected to spin ordering and can be described using a simple spin-density wave mean-field theory (Slater regime). The characteristic coupling u^* separating these two regimes is also the one at which the crossover from a liquid to an insulating state takes place in the paramagnetic state. The Slater and Mott-Heisenberg regimes are connected by a smooth crossover.

5.1.2 From repulsion to attraction

There is actually a direct formal analogy between this physics and that of the BCS-BEC crossover in the Hubbard model with an *attractive interaction*. Indeed, on a bipartite lattice (i.e. a lattice made of two sublattice A and B) with nearest-neighbour hopping, one can perform the following symmetry operation:

$$c_{i\uparrow} \rightarrow \widetilde{c}_{i\uparrow} \ , \ c_{i\downarrow} \rightarrow (-1)^i \widetilde{c}^{\dagger}_{i\downarrow} \tag{5.1}$$

with $(-1)^i = +1$ on the A-sublattice and $= -1$ on the B-sublattice. At half-filling, this symmetry simply changes the sign of the coupling U, hence establishing an exact connection between the two cases. Long-range AF order along the x- or y-axis is mapped onto superconducting long-range order, while AF order along the z-axis is mapped onto a charge-density wave state in which pairs reside preferentially on one sublattice. The two types of ordering are degenerate at half-filling in the attractive case. The BCS regime of the attractive case maps onto the Slater regime of the repulsive one, and the BEC regime onto the Mott-Heisenberg one. In fact, the symmetry also maps the attractive model away from half-filling onto the repulsive model at half-filling in a uniform magnetic field.

Chapter 6

Complementary Material - Technical Notes - Useful Books

6.1 Appendixes and Technical notes

- Introductory lecture on second quantization (C.Mora) and TD (appended)
- Some technical notes (AG) from the 2011 lectures (appended)

6.2 Useful General Books

The list is kept short on purpose.

- **Books on the many-body problem.** Closest to these lectures is: H. Bruus and K. Flensberg *Many-Body Quantum Theory in Condensed Matter Physics - An Introduction*, Oxford University Press; For a detailed presentation of the more technical aspects of the many-body problem, the standard reference is: G. D. Mahan, *Many-Particle Physics* (Kluwer, 3rd edition).
- **Basic book on solid-state physics.** The classic reference is Ashcroft and Mermin. See also: P.W Anderson *Concepts in Solids: Lectures on the Theory of Solids* World Scientific. (A very simple book on the concept of elementary excitations).

6.3 Books on more specialized or advanced topics

The following books mostly deal with topics which are beyond the scope of these lectures, and are included here for the curious and hardy minds, and for future use...

- **Landau theory of Fermi Liquids.** Abrikosov, Gorkov, Dzyaloshinski *Methods of quantum field theory in statistical physics* Dover ed.; D.Pines and P.Nozieres *The theory of quantum liquids, Vol I* Benjamin ed.; R. Shankar, *Renormalization-group approach to interacting fermions* Reviews of Modern Physics, Vol.66, (1994) p.129 (gives a renormalization-group point of view on the foundations of Fermi Liquid Theory).

- **Functional-integral Methods for bosons and fermions** (formal aspects). J.F. Negele et H. Orland *Quantum many-particle physics* Addison-Wesley.

- **One-dimensional quantum systems.** T. Giamarchi, *Quantum Physics in One Dimension*, Oxford University Press (a great book !); A. M. Tsvelik, *Quantum Field Theory in Condensed Matter Physics* (emphasizes field-theory methods - mostly $1+1$-dimensional but not exclusively.

- **Quantum Magnetism.** A. Auerbach, *Interacting Electrons and Quantum Magnetism*, Springer Verlag.

- **Quantum Phase Transitions.** Sachdev, *Quantum Phase Transitions*, Cambridge University Press (another great book !).

- **Superconductivity.** J. R. Schrieffer, *Theory of Superconductivity*, Perseus Books ed.; P. G. de Gennes, *Superconductivity of Metals and Alloys*, Perseus Books ed.

Concepts Fondamentaux de la Physique

Introduction to Second Quantization

Christophe Mora

Contents

Part of the complexity in the many-body problem - systems involving many particles - comes from the indistinguishability of identical particles, fermions or bosons. Calculations in first quantization thus involve the cumbersome (anti-)symmetrization of wavefunctions.

Second quantization is an efficient technical tool that describes many-body systems in a compact and intuitive way.

1 Preliminaries

Before entering the details of second quantization, it is worth drawing a clear distinction between the single-particle and the many-particle Hilbert spaces.

1.1 Single-particle Hilbert space

Consider a single particle described by the hamiltonian $\hat{h}$ acting on the Hilbert space $\mathcal{H}_1$. $\mathcal{H}_1$ is generated by the complete set of eigenfunctions $|\lambda\rangle$ ($\lambda = \mathbf{k}, \sigma, \nu, \ldots$)

$$\hat{h}|\lambda\rangle = \varepsilon_\lambda |\lambda\rangle,$$

with the eigenvalues ε_λ. The identity operator in $\mathcal{H}_1$ is given by the completeness relation $\mathbb{1} = \sum_\lambda |\lambda\rangle\langle\lambda|$.

Examples:

1. single particle in free space, $\hat{h} = -\hbar^2\nabla^2/(2m)$. The eigenfunctions are labeled by the wavevectors $\mathbf{k}$ with $\psi_k(\mathbf{r}) = \langle \mathbf{r}|\mathbf{k}\rangle = \frac{e^{i\mathbf{k}\cdot\mathbf{r}}}{\sqrt{V}}$ and the energies $\varepsilon_k = \hbar^2 k^2/2m$.

2. spin 1/2 in a magnetic field, $\hat{h} = -BS^z$. The Hilbert space has dimension 2, generated by the eigenstates $|\uparrow\rangle$ and $|\downarrow\rangle$ of the spin operator S^z.

The basis of two-particle states, given by the set of (anti-)symmetrized functions, + for bosons and − for fermions,

$$\psi_{\lambda,\nu}(1,2) = \frac{1}{\sqrt{2}}\left[\varphi_\lambda(1)\,\varphi_\nu(2) \pm \varphi_\lambda(2)\,\varphi_\nu(1)\right],$$

is built out of the single-particle states $\varphi_\lambda(1) = \langle 1|\lambda\rangle$. The corresponding Hilbert space[1] is denoted $\mathcal{F}_2$.

1.2 Many-particle Hilbert space

We first discuss fermions. Following the two-particle case, the set of antisymmetrized Slater determinants

$$\psi_{\lambda_1,\ldots,\lambda_N}(1,\ldots,N) = \frac{1}{\sqrt{N!}}\sum_{P\in S_N}(-1)^P \varphi_{\lambda_1}(P_1)\ldots\varphi_{\lambda_N}(P_N), \tag{1}$$

where the summation runs over all permutations of $\{1,\ldots,N\}$, forms the basis[2] of the Hilbert space $\mathcal{F}_N$. In the bosonic case, the basis is obtained from symmetrized states, *i.e.* Eq. (1) where $(-1)^P$ is replaced by 1.

The hamiltonian may describe independent particles in which case

$$\hat{H} = \sum_{i=1}^{N} \hat{h}^{(i)},$$

where each piece $\hat{h}^{(i)}$ acts only on the particle i.

Examples:

1. for particles in free space, $\hat{H} = \sum_i \mathbf{p}_i^2/(2m)$.
2. for an assembly of N distinguishable spins in a magnetic field, $\hat{H} = -B\sum_{i=1}^{N} S_i^z$. The Hilbert space has dimension 2^N and symmetrization is not required.

Interactions between particles can be added, $\hat{H} = \sum_i \hat{h}^{(i)} + \hat{V}$, where $\hat{V}$ includes all multi-particle interactions. For example, Coulomb interactions read

$$\hat{V}_{\text{Coulomb}} = \sum_{i=1}^{N}\sum_{j>i}^{N} \frac{e^2}{4\pi\varepsilon_0}\frac{1}{|\mathbf{r}_i - \mathbf{r}_j|}. \tag{2}$$

2 Basics of second quantization

So far, we have introduced and discussed the many-body problem in the language of first quantization. Second quantization corresponds to a different labelling of the basis of states Eq. (1) together with the introduction of creation and annihilation operators that connect spaces with different numbers of particles.

[1] Restricted to (anti-)symmetrized wavefunctions, $\mathcal{F}_2$ is a subset of the larger space $\mathcal{H}_1 \otimes \mathcal{H}_1$.

[2] A different choice for the set of single-particle states $|\lambda\rangle$ gives, using Eq. (1), a different many-particle basis that nevertheless spans the same Hilbert space $\mathcal{F}_N$.

2.1 Occupation number representation

Since identical particles are indistinguishable, it is not possible, for a state of the form Eq. (1), to ascribe a definite single-particle state to a given particle. Therefore, instead of focusing on the wavefunction of each particle individually, one can reverse the perspective and characterize the states of Eq. (1) by the set of single-particle states $\{\lambda_1, \ldots, \lambda_N\}$ that are occupied by particles, all other single-particle states being empty.

In terms of notations, $|\{n_\lambda\}\rangle$ represents $|\psi_{\lambda_1,\ldots,\lambda_N}\rangle$[3] with, for fermions, $n_\lambda = 1$ for $\lambda = \lambda_i$, $i = 1 \ldots N$, and $n_\lambda = 0$ otherwise. The state can be written schematically as

$$|\{n_\lambda\}\rangle = |0 \ldots \overset{\lambda_1}{1} \ldots 0 \ldots \overset{\lambda_2}{1} \ldots 0 \ldots (\ldots) \overset{\lambda_N}{1}\rangle, \tag{3}$$

where it is explicitly specified on the right-hand-side which states are occupied and which state are empty.

Bosonic states have similar expressions although the occupation numbers n_λ can take values larger than 1, for example

$$|\{n_\lambda\}\rangle = |0 \ldots \overset{\lambda_1}{5} \ldots 0 \ldots \overset{\lambda_2}{1} \ldots 0 \ldots (\ldots) \overset{\lambda_N}{7}\rangle, \tag{4}$$

for $n_{\lambda_1} = 5$, $n_{\lambda_2} = 1$, ..., $n_{\lambda_N} = 7$.

2.2 Creation and annihilation operators

The constraint on the number of particles, $\sum_\lambda n_\lambda = N$, can be released by working in the extended Hilbert space

$$\mathcal{F} = \bigoplus_{N=0}^{+\infty} \mathcal{F}_N,$$

called the Fock space. Here, $\mathcal{F}_1 = \mathcal{H}_1$ is the single-particle Hilbert space, $\mathcal{F}_0$ contains a unique vacuum state, often noted $|0\rangle$, in which no particle is present.

In the Fock space, creation operators are introduced that raise the number of particles in a given single-particle state by 1. For fermions, it reads

$$c^\dagger_{\lambda_1} |0 \ldots \overset{\lambda_1}{0} \ldots 0 \ldots \overset{\lambda_2}{1} \ldots 0 \ldots (\ldots) \overset{\lambda_N}{1}\rangle = |0 \ldots \overset{\lambda_1}{1} \ldots 0 \ldots \overset{\lambda_2}{1} \ldots 0 \ldots (\ldots) \overset{\lambda_N}{1}\rangle,$$

while particle creation in a single-particle state that is already occupied gives zero,

$$c^\dagger_{\lambda_2} |0 \ldots \overset{\lambda_1}{1} \ldots 0 \ldots \overset{\lambda_2}{1} \ldots 0 \ldots (\ldots) \overset{\lambda_N}{1}\rangle = 0.$$

The annihilation operator c_λ, lowering the number by 1, is the hermitian conjugate of $c^\dagger_\lambda$. The full basis of the Fock space $\mathcal{F}$ is in fact generated by creation operators applied on the vacuum state, namely $|n_{\lambda_1} = 1, \ldots, n_{\lambda_N} = 1\rangle = c^\dagger_{\lambda_1} \ldots c^\dagger_{\lambda_N} |0>$.

The antisymmetric properties of the basis states (Slater determinants) $|n_{\lambda_1} \ldots n_{\lambda_N}\rangle$ are ensured by the anticommutation relations

$$\{c_\alpha, c_\beta\} = c_\alpha c_\beta + c_\beta c_\alpha = 0, \qquad \{c_\alpha, c^\dagger_\beta\} = \delta_{\alpha,\beta}. \tag{5}$$

The product $\hat{n}_\lambda = c^\dagger_\lambda c_\lambda$ gives the number of fermions occupying the state $|\lambda\rangle$,

$$c^\dagger_\lambda c_\lambda |\{n_\alpha\}\rangle = n_\lambda |\{n_\alpha\}\rangle$$

where $n_\lambda = 0$ or 1.

[3] $\psi_{\lambda_1,\ldots,\lambda_N}(1, \ldots, N) = \langle 1, \ldots, N | \psi_{\lambda_1,\ldots,\lambda_N}\rangle$.

2.3 Bosons

There are only slight differences in the way second quantization works for fermions and for bosons. In the case of bosons, the basis states are symmetrized functions and the number of bosons in a given single-particle state is not restricted. These properties are ensured by the commutation relations

$$[b_\alpha, b_\beta] = b_\alpha b_\beta - b_\beta b_\alpha = 0, \qquad [b_\alpha, b_\beta^\dagger] = \delta_{\alpha,\beta}, \tag{6}$$

with the (annihilation) creation operators (b_α) $b_\alpha^\dagger$. From Eq. (6), one can prove[4] that

$$\begin{aligned} b_\lambda^\dagger |n_\lambda\rangle &= \sqrt{n_\lambda + 1}\,|n_\lambda + 1\rangle \\ b_\lambda |n_\lambda\rangle &= \sqrt{n_\lambda}\,|n_\lambda - 1\rangle \end{aligned} \tag{7}$$

such that $\hat{n}_\lambda = b_\lambda^\dagger b_\lambda$ is indeed the number operator, $\hat{n}_\lambda |n_\lambda\rangle = n_\lambda |n_\lambda\rangle$.

3 Representation of operators

The complexity associated with wavefunction (anti)symmetrization has been reduced, in the formalism of second quantization, to the surprisingly simple commutation relations, Eq. (5) for fermions and Eq. (6) for bosons. Had the usual operators of the theory complicated expressions in terms of creation/annihilation operators, this would not be very useful. However, as we shall see below, the hamiltonian as well as standard operators do have simple expressions in second quantization.

3.1 Change of basis and the field operator

Starting with the expression $|\lambda\rangle = c_\lambda^\dagger |0\rangle$, one can insert the closure relation $\mathbb{1} = \sum_\lambda |\lambda\rangle\langle\lambda|$ to derive the transformation law for the creation/annihilation operators

$$c_\alpha^\dagger = \sum_\lambda \langle\lambda|\alpha\rangle\, c_\lambda^\dagger, \qquad c_\alpha = \sum_\lambda \langle\alpha|\lambda\rangle\, c_\lambda, \tag{8}$$

from one basis to another. Hence, the change of basis only requires the calculation of matrix elements $\langle\alpha|\lambda\rangle$ involving single-particle states.

By convention, the field operator $\Psi(\mathbf{r})$ in a continuous problem is associated to the basis of position states $|\mathbf{r}\rangle$,

$$\Psi(\mathbf{r}) = \sum_\lambda \langle\mathbf{r}|\lambda\rangle\, c_\lambda. \tag{9}$$

Using Eq. (5) and Eq. (6), one finds the commutation relation

$$\begin{aligned} \{\Psi(\mathbf{r}), \Psi(\mathbf{r}')\} &= 0, & \{\Psi(\mathbf{r}), \Psi^\dagger(\mathbf{r}')\} &= \delta(\mathbf{r} - \mathbf{r}'), & &\text{fermions,} \\ [\Psi(\mathbf{r}), \Psi(\mathbf{r}')] &= 0, & [\Psi(\mathbf{r}), \Psi^\dagger(\mathbf{r}')] &= \delta(\mathbf{r} - \mathbf{r}'), & &\text{bosons.} \end{aligned} \tag{10}$$

The total number of particles (fermions or bosons) is then given by

$$\hat{N} = \sum_\lambda c_\lambda^\dagger c_\lambda = \int d^d r\, \hat{\rho}(\mathbf{r}) \tag{11}$$

[4] The states $|n_\lambda\rangle$ are chosen to be normalized to 1.

where the local density operator $\hat{\rho}(\mathbf{r}) = \Psi^\dagger(\mathbf{r})\Psi(\mathbf{r})$ has been introduced.

Example: The transformation to the Fourier momentum representation reads

$$\Psi(\mathbf{r}) = \frac{1}{\sqrt{V}} \sum_{\mathbf{k}} e^{i\mathbf{k}\cdot\mathbf{r}}\, c_{\mathbf{k}}, \tag{12}$$

where $c_{\mathbf{k}}$ destroys a particle with momentum $\mathbf{k}$. The total number of particle is given by $\hat{N} = \sum_{\mathbf{k}} c^\dagger_{\mathbf{k}} c_{\mathbf{k}}$.

3.2 Representation of one-body and two-body operators

Single-particle or one-body operators have the form $\hat{O}^{(1)} = \sum_{i=1}^{N} \hat{o}^{(1)}[i]$ in first quantization, where $\hat{o}^{(1)}[i]$ is a single-particle operator acting on the ith particle. In the language of second quantization, they take the form

$$\hat{O}^{(1)} = \sum_{\alpha,\beta} \langle\alpha|\hat{o}^{(1)}|\beta\rangle\, c^\dagger_\alpha c_\beta, \tag{13}$$

with the matrix elements $\langle\alpha|\hat{o}^{(1)}|\beta\rangle = \int d1\, d2\ \varphi^*_\alpha(1)\langle 1|\hat{o}^{(1)}|2\rangle\varphi_\beta(2)$.

Examples:

1. The kinetic energy operator $\hat{T} = \sum_i \mathbf{p}_i^2/(2m)$, describing independent particles, reads in second quantization

$$\hat{T} = \sum_{\mathbf{k}} \frac{\hbar^2 k^2}{2m}\, c^\dagger_{\mathbf{k}} c_{\mathbf{k}}, \tag{14}$$

i.e. it is diagonal in the momentum basis. An alternative expression involving the field operator is

$$\hat{T} = \int d^d r\, \Psi^\dagger(\mathbf{r})\, \frac{(\hbar\nabla/i)^2}{2m}\, \Psi(\mathbf{r}) = \int d^d r\, \frac{\hbar^2}{2m}\, \nabla\Psi^\dagger(\mathbf{r})\cdot\nabla\Psi(\mathbf{r}). \tag{15}$$

2. Tight-binding models are simplified band models for electrons in solids where only neighboring sites hybridize. A particularly simple example is given by the hamiltonian

$$\hat{H} = -t \sum_{\langle i,j\rangle} \left(c^\dagger_i\, c_j + c^\dagger_j\, c_i \right), \tag{16}$$

where $c^\dagger_i$ creates an electron on site i and $\langle i,j\rangle$ denotes neighboring sites. The product $c^\dagger_i\, c_j$ describes intuitively the hopping of an electron from site j to site i: one electron is annihilated on site j while a novel electron appears on site i. The hamiltonian Eq. (16) is diagonalized by going to the Fourier space $c_{\mathbf{k}} = \frac{1}{\sqrt{N_s}} \sum_i e^{-i\mathbf{k}\cdot\mathbf{r}_i}\, c_i$ (N_s is the number of sites of the lattice), with the result $\hat{H} = \sum_{\mathbf{k}} \varepsilon_{\mathbf{k}} c^\dagger_{\mathbf{k}} c_{\mathbf{k}}$. In one dimension, $\varepsilon_k = -2t\cos(ka)$, a being the lattice spacing.

We now consider a two-body operator such as the Coulomb interaction of Eq. (2). In first quantization, it has the form

$$\hat{O}^{(2)} = \frac{1}{2} \sum_{i\neq j} \hat{o}^{(2)}[i,j], \tag{17}$$

where $\hat{o}^{(2)}[i,j]$ accounts for pair interactions. In second quantization, it reads[5]

$$\hat{O}^{(2)} = \frac{1}{2} \sum_{\alpha,\beta,\gamma,\delta} \langle \alpha\, \beta | \hat{o}^{(2)} | \gamma\delta \rangle c_\alpha^\dagger c_\beta^\dagger c_\delta c_\gamma, \tag{18}$$

with the matrix elements

$$\langle \alpha\, \beta | \hat{o}^{(2)} | \gamma\delta \rangle = \int d1\, d2\, \varphi_\alpha^*(1) \varphi_\beta^*(2) \hat{o}^{(2)}[1,2] \varphi_\gamma(1) \varphi_\delta(2). \tag{19}$$

Example: Electron-electron Coulomb interaction is given in second quantization by

$$\hat{V}_{\text{Coulomb}} = \frac{1}{2} \sum_{\sigma_1,\sigma_2} \int d\mathbf{r}_1\, d\mathbf{r}_2\, \frac{e^2}{4\pi\varepsilon_0 |\mathbf{r}_1 - \mathbf{r}_2|}\, \Psi_{\sigma_1}^\dagger(\mathbf{r}_1) \Psi_{\sigma_2}^\dagger(\mathbf{r}_2) \Psi_{\sigma_2}(\mathbf{r}_2) \Psi_{\sigma_1}(\mathbf{r}_1), \tag{20}$$

in terms of the field operator $\Psi_\sigma(\mathbf{r})$. Here the spin σ of electrons has been included. After going to the Fourier momentum representation of Eq. (12), one obtains the alternative expression

$$\hat{V}_{\text{Coulomb}} = \frac{1}{2V} \sum_{\sigma_1,\sigma_2} \sum_{\mathbf{q},\mathbf{k}_1,\mathbf{k}_2} v(q)\, c_{\mathbf{k}_1+\mathbf{q},\sigma_1}^\dagger c_{\mathbf{k}_2-\mathbf{q},\sigma_2}^\dagger c_{\mathbf{k}_2,\sigma_2} c_{\mathbf{k}_1,\sigma_1}$$

with the Fourier transform of the Coulomb pair potential $v(q) = e^2/(\varepsilon_0\, q^2)$.

[5]Note the ordering of indices which, in the product of annihilation operators, is reversed with respect to the ordering in the matrix element.

Theory of Condensed Matter

Exercises on second quantization

Xavier Leyronas, Christophe Mora

1 Starters

1. For $\alpha \neq \beta$, compute the matrix element $\langle 0|c_\alpha c_\beta c_\alpha^\dagger c_\beta^\dagger|0\rangle$ for fermions and for bosons.
2. Consider free fermions with spin 1/2 in a box of volume V. Write the hamiltonian $\hat{H}_0$ in second quantization in the Fourier momentum representation.
   (a) Write the expression of the ground state $|\mathrm{FS}\rangle$.
   (b) Compute the following quantities
   $$\langle \hat{n}_{k\sigma}\rangle = \langle \mathrm{FS}|c_{k\sigma}^\dagger c_{k\sigma}|\mathrm{FS}\rangle, \qquad E_0 = \langle \mathrm{FS}|\hat{H}_0|\mathrm{FS}\rangle, \qquad N_0 = \langle \mathrm{FS}|\hat{N}|\mathrm{FS}\rangle,$$
   in the thermodynamic limit $V \to +\infty$.
3. In the case of fermions, prove that
   $$c_\alpha^\dagger|\{n_\beta\}\rangle = \begin{cases} (-1)^{\sum_{\beta<\alpha}} |n_1\, n_2 \ldots \overset{\alpha}{1}\; n_{\alpha+1} \ldots n_N\rangle & \text{if } n_\alpha = 0 \\ 0 & \text{if } n_\alpha = 1 \end{cases} \tag{1}$$
   and
   $$c_\alpha|\{n_\beta\}\rangle = \begin{cases} 0 & \text{if } n_\alpha = 0 \\ (-1)^{\sum_{\beta<\alpha}} |n_1\, n_2 \ldots \overset{\alpha}{0}\; n_{\alpha+1} \ldots n_N\rangle & \text{if } n_\alpha = 1 \end{cases} \tag{2}$$
4. Show that the change of basis
   $$c_\beta^\dagger = \sum_\alpha U_{\beta\alpha} c_\alpha^\dagger,$$
   preserves the canonical commutation relations iff U is a unitary matrix. Is $U_{\beta\alpha} = \langle\beta|\alpha\rangle$ a unitary matrix ? Show that the expression of the number operator $\hat{N} = \sum_\alpha c_\alpha^\dagger c_\alpha$ is not modified by the above transformation.
5. For bosons, show that
   $$|n_1\, n_2 \ldots\rangle = \prod_i \frac{(b_i^\dagger)^{n_i}}{\sqrt{n_i!}}|0\rangle.$$
6. Compute the commutator $[\hat{H}_0, \hat{N}]$ for free fermions. What is the meaning of the result ? Is it modified when interactions are taken into account ?
7. Consider spinless free fermions or free bosons.
   (a) Derive the expression $\hat{H}_0 = \sum_k \varepsilon_k c_k^\dagger c_k$ from $\hat{H}_0 = -(\hbar^2/2m)\int dr\, \psi^\dagger(r)\nabla^2\psi(r)$.
   (b) Derive the expression of the Coulomb pair potential in the momentum representation starting from $\hat{V}_{\mathrm{Coulomb}} = \frac{1}{2}\sum_{\sigma_1,\sigma_2}\int dr_1\, dr_2\, V(r_1 - r_2)\, \Psi_{\sigma_1}^\dagger(r_1)\Psi_{\sigma_2}^\dagger(r_2)\Psi_{\sigma_2}(r_2)\Psi_{\sigma_1}(r_1)$.
8. Consider the one-dimensional tight-binding model ($t > 0$)
   $$\hat{H} = -t\sum_i \left(c_i^\dagger\, c_{i+1} + \mathrm{h.c.}\right), \tag{3}$$
   with periodic boundary conditions $c_{N_s+1} = c_1$, describing the hopping of electrons on a lattice of N_s sites with lattice spacing a. Diagonalize the hamiltonian by going to the Fourier space and show that the eigenenergies are given by
   $$\varepsilon_k = -2t\cos(ka).$$
   What are the admissible values for the wavevector k ?

9. The local density operator is given for a single particle by $\hat{\rho}(\mathbf{r}) = |\mathbf{r}\rangle\langle\mathbf{r}|$. Give the expression of $\hat{\rho}(\mathbf{r})$ in second quantization in a given basis $|\varphi_\lambda\rangle$ of one-particle states. Give $\hat{\rho}(\mathbf{r})$ in the basis of position states $|\mathbf{r}\rangle$. In the basis of momentum states $|\mathbf{k}\rangle$, give $\hat{\rho}(\mathbf{r})$ and then its Fourier transform

$$\hat{\rho}(\mathbf{q}) = \int d\mathbf{r}\, \hat{\rho}(\mathbf{r}) e^{-i\mathbf{q}\cdot\mathbf{r}}$$

2 Spin operator

We consider fermions with spin 1/2. We denote by $\alpha = \uparrow, \downarrow$ the spin component. The spin operator of the many-body system assumes the form

$$\hat{\mathbf{S}} = \sum_\lambda c^\dagger_{\lambda\alpha'} \frac{\sigma_{\alpha'\alpha}}{2} c_{\lambda\alpha} \tag{4}$$

where $\sigma = (\sigma_x, \sigma_y, \sigma_z)$ is a vector composed by the standard Pauli matrices [1], and λ denotes the set of additional quantum numbers (wavevector, lattice site index, etc).

1. Forget about spin for one moment and consider a finite Hilbert space with N one-particle states. We use the notation $c^\dagger = (c^\dagger_1, c^\dagger_2, \ldots, c^\dagger_N)$ as a vector with N entries. Prove the following identity

   $$[c^\dagger\, A\, c, c^\dagger\, B\, c] = c^\dagger\, [A, B]\, c$$

   where A and B are $N \times N$ matrices.
2. Use the previous result to show that the spin operator in Eq. (4) satisfies the commutation relations of the Lie group SU(2).
3. Can we say something specific about $\hat{\mathbf{S}}^2$?
4. Give the spin raising and lowering operators $\hat{S}^\pm = \hat{S}_x \pm i\hat{S}_y$ in terms of creation and annihilation operators.

We take the Hubbard model in the atomic limit : a single site governed by the hamiltonian

$$\hat{H} = \varepsilon_d(\hat{n}_\uparrow + \hat{n}_\downarrow) + U\, \hat{n}_\uparrow \hat{n}_\downarrow$$

where $\hat{n}_\sigma = d^\dagger_\sigma d_\sigma$.

5. Give the size of the corresponding Hilbert space.
6. Diagonalize the hamiltonian.
7. Precise the spin for each eigenstate.

3 Hartree-Fock

We consider a gas of N electrons with spin 1/2. The hamiltonian includes kinetic and Coulomb energies, $\hat{H} = \hat{T} + \hat{V}$ or

$$\hat{H} = \sum_{\sigma,\mathbf{k}} \varepsilon_k\, c^\dagger_{\mathbf{k}\sigma} c_{\mathbf{k}\sigma} + \frac{1}{2V} \sum_{\sigma_1,\sigma_2} \sum_{\mathbf{q},\mathbf{k}_1,\mathbf{k}_2} \frac{e^2}{\varepsilon_0\, q^2}\, c^\dagger_{\mathbf{k}_1+\mathbf{q},\sigma_1} c^\dagger_{\mathbf{k}_2-\mathbf{q},\sigma_2} c_{\mathbf{k}_2,\sigma_2} c_{\mathbf{k}_1,\sigma_1}. \tag{5}$$

This hamiltonian can not be diagonalized. We shall therefore treat the Coulomb interaction $\hat{V}$ in perturbation theory.

1. What is the ground state of the system in the absence of $\hat{V}$?

---

1. $$\sigma_x = \begin{pmatrix} 0 & 1 \\ 1 & 0 \end{pmatrix} \qquad \sigma_y = \begin{pmatrix} 0 & -i \\ i & 0 \end{pmatrix} \qquad \sigma_z = \begin{pmatrix} 1 & 0 \\ 0 & -1 \end{pmatrix}$$

2. Show that the correction to the ground state energy, to leading order in $\hat{V}$, has two contributions : a direct Hartree term, which in this case is infinite, and an exchange Fock term.
3. Compute the Fock term using the identity

$$\mathcal{V}_q = \sum_{\mathbf{k}} \theta[\varepsilon_F - \varepsilon_{\mathbf{k}}]\theta[\varepsilon_F - \varepsilon_{\mathbf{k}+\mathbf{q}}] = \frac{4\pi k_F^3}{3}\left[1 - \frac{3}{4}\frac{q}{k_F} + \frac{1}{16}\left(\frac{q}{k_F}\right)^3\right] \qquad \text{for} \quad |\mathbf{q}| < 2k_F$$

and zero for $|\mathbf{q}| \geq 2k_F$. Find the result

$$\frac{\delta E}{V} = -\frac{k_F^4}{4\pi^3}\frac{e^2}{4\pi\varepsilon_0}.$$

4 Finite temperature and thermodynamics

We recall that the partition function Z in the grand canonical ensemble is given by

$$Z = \mathrm{Tr} e^{-\beta(\hat{H}-\mu\hat{N})}$$

where the trace is taken over all states of the many-body Hilbert space. μ denotes here the chemical potential. The mean value of an operator $\hat{O}$ acting in the many-body Hilbert space is then given by

$$\langle \hat{O} \rangle = \frac{1}{Z}\,\mathrm{Tr}\left[\hat{O}\, e^{-\beta(\hat{H}-\mu\hat{N})}\right].$$

1. Suppose that the hamiltonian is diagonal in the occupation number for some particular one-particle basis,

$$\hat{H} = \sum_{\lambda} \varepsilon_\lambda \hat{n}_\lambda.$$

This implies in passing that particles are independent, *i.e.* not interacting. Show that the partition function factorizes as $Z = \prod_\lambda Z_\lambda$.
2. Give the expression of Z_λ for fermions and for bosons.
3. Compute $\langle \hat{n}_\lambda \rangle$ for fermions and for bosons. Which distributions do we find ?

MASTER CFP – Cours 1 – AG – 12/09/11

1. One-particle wavefunctions

$\hat{H} = \hat{H}_0 + \hat{H}_{int}$ $\quad \hat{H}_0 = \sum_{i=1}^{N} \hat{h}_0^{(i)}$ indep. particles

$\hat{h}|\alpha\rangle = \varepsilon_\alpha |\alpha\rangle$ $\quad$ w.f $\quad \langle r|\alpha\rangle = \varphi_\alpha(r)$

α a collective index (all nec. quantum numbers)

Examples :

1. Free particles in free space $\hat{h} = \frac{\hat{p}^2}{2m} \equiv -\frac{\hbar^2\nabla^2}{2m}$

Plane waves momentum $\vec{k}$; spin σ

$\varphi_{\vec{k}}(\vec{r}) = \frac{1}{\sqrt{\Omega}} e^{i\vec{k}\cdot\vec{r}}$ $\quad \varepsilon_{\vec{k}} = \frac{\hbar^2\vec{k}^2}{2m}$

2. Particles in a periodic lattice potential –

e.g. electrons in crystal lattice

$\hat{h} = -\frac{\hbar^2\nabla^2}{2m} + V(\vec{r})$

Naively : $V(\vec{r}) = -\sum_m \frac{e^2}{4\pi\varepsilon_0} \frac{Z_m}{|\vec{r} - \vec{R}_m|} \equiv V_c(\vec{r})$

In fact $V(\vec{r}) \equiv V_{eff}(\vec{r}) = V_c(\vec{r}) + V_H(\vec{r}) + V_{xc}(\vec{r})$

or : atoms in optical lattice. → (1)

$V_{latt}(\vec{r}) = V(x) + V(y) + V(z)$ simplest case (cubic)

$V(x) = V_0 \sin^2(k_L x)$ $\quad k_L = \frac{2\pi}{\lambda}$ $\quad V_0$: laser amplit.

General properties of w.f in periodic potential

Lattice = Bravais lattice + base

ex. honeycomb (graphene) = triangular + 2-site base

Unit-cell : pave space w/ lattice translations $\vec{T}$

Material : need positions of atoms in unit-cell

Wave-vectors : reciprocal space (Fourier for discrete translations).

Reciprocal ('dual') lattice :

$\vec{e}_i \cdot \vec{e}^*_j = 2\pi \delta_{ij}$ $\quad \vec{G} = \sum_i m_i \vec{e}^*_i$ rec. latt. vector

G's are the vectors involved in Fourier of lattice-periodic function

$f(\vec{r}+\vec{T}) = f(\vec{r}) \longrightarrow f(\vec{r}) = \sum_G \hat{f}_G e^{i\vec{G}\cdot\vec{r}}$

Unit-cell of reciprocal lattice: Brillouin zone (BZ)

ex: cubic lattice spacing a

$\hat{e}_x = a\hat{x}$; $\hat{e}^*_x = \frac{2\pi}{a}\hat{x}$; $BZ = \left[-\frac{\pi}{a}, \frac{\pi}{a}\right]^d$

$\Omega \cdot \Omega_{BZ} = (2\pi)^d$ (general)

Bloch's theorem (reminder)

1-particle wfs of $\hat{h}$ are of the form :

$$\varphi_{\vec{k}v}(\vec{r}) = e^{i\vec{k}\cdot\vec{r}} u_{\vec{k}v}(\vec{r}) \quad \text{with } u_{\vec{k}v}(\vec{r}+\vec{T}) = u_{\vec{k}v}(\vec{r}) \text{ (lattice-period.)}$$

Physical meaning $\longrightarrow$ [T]

Here: $\vec{k} \in BZ$ 'quasi-momentum' (or 'crystal-m)

ν : band index : discrete label of eigenstate

$u_{k\nu}(r) = \sum_G \hat{u}^G_{k\nu} e^{iG.r}$

Hence $\varphi_{k\nu} = \sum_G e^{i(\vec{k}+\vec{G}).\vec{r}} \hat{u}^G_{k\nu}$: contains all $\vec{k}+\vec{G}$

Wannier function centered on $\vec{R}$ (lattice site)

$$|w_{\vec{R}\nu}\rangle \equiv \int \frac{d\vec{k}}{\Omega_{BZ}} e^{-i\vec{k}.\vec{R}} |\varphi_{\vec{k}\nu}\rangle$$

Exos: $w_\nu(\vec{r}-\vec{R}) = \int \frac{dk}{\Omega_{BZ}} e^{ik(r-R)} u_{k\nu}(r)$ depends only on $\vec{r}-\vec{R}$

$$\langle w^R_\nu | w^{R'}_{\nu'} \rangle = \delta_{\nu\nu'} \delta_{RR'}$$

w^R_ν localised around $\vec{R}$ $\longrightarrow$ T

* Admissible values of $\vec{k}$:

PBC $\rightarrow$ $k_x = \frac{2\pi}{L_x} m_x$; $m_x \in \mathbb{Z}$ etc.

Finely spaced but discrete for finite L

$\longrightarrow$ continuous $\vec{k} \in BZ$ for infinite volume $\Omega \to \infty$

Discrete $\sum_{\vec{k}}$ $\longrightarrow \frac{\Omega}{(2\pi)^d} \int d\vec{k} (\dots)$ as $\Omega \to \infty$

Bands: Two important limits –

1– Weak potential ('liaisons faibles')

ex: D = 1 –

Fold parabola $\frac{\hbar^2 k^2}{2m}$ according to $\left[-\frac{\pi}{a}, \frac{\pi}{a}\right]$ BZ

→ T

Open gaps at degeneracy points

(1st order p.t in V(r) not valid @ these points)

→ Gaps for $(\vec{k}+\vec{G})^2 = \vec{k}^2$ Bragg condition

Effect of V largest close to these points

→ eff mass in semicon ≠ m (typ ~ $m/10$).

2– Tight-binding ('liaisons fortes')

. Atoms far away → atomic levels broaden but ~ do not mix.

. Deep optical lattice –

Single atomic level: ε_0 ; w.f $\chi(\vec{r})$

On site $\vec{R}_n = na$ $|\chi_n\rangle$ $\langle r|\chi_n\rangle = \chi(r - R_n)$

Assume / Approx:

$\langle \chi_n | \hat{h} | \chi_n \rangle = \bar{\varepsilon}_0$ ren. at. level

$\langle \chi_n | \hat{h} | \chi_m \rangle = -t$ for n.n only (can extend)

$\langle \chi_n | \chi_m \rangle = \delta_{nm}$ (neglect overlap – can orthonormalize) –

$$\hat{h} = \bar{\varepsilon}_0 \sum_n |x_n\rangle\langle x_n| - t \sum_{\langle n,m \rangle} |x_n\rangle\langle x_m|$$

Explicitly:

$$\begin{bmatrix} \bar{\varepsilon}_0 & -t & & & -t \\ -t & \ddots & \ddots & & \\ & \ddots & \ddots & -t & \\ & & -t & \bar{\varepsilon}_0 & \\ -t & & & & \end{bmatrix}$$

← PBC on ring!

Exo: Show that

$$\varepsilon_k = \bar{\varepsilon}_0 - 2t\cos(ka)$$

Band $[-2t, +2t]$ Width $W = 4t$

Wavefunctions:

$$\varphi_k(x) = \frac{1}{\sqrt{N_s}} \sum_{n=1}^{N_s} e^{ikna} \chi(x - na)$$

$$= e^{ikx} \underbrace{\frac{1}{\sqrt{N_s}} \sum_n e^{-ik(x-na)} \chi(x-na)}_{u_k(x) \text{ Bloch funct.}}$$

Bottom of band → bonding ($t > 0$)
Top " " → antibonding ✓

Generalisation to cubic lattice:

$$\varepsilon_{\vec{k}} = \bar{\varepsilon}_0 - 2t \sum_{\mu=1}^{d} \cos(k_\mu a) \qquad W = 4dt$$

Ground-state and excitations
(independent particles)

Ground-state : Fermi sea

Fill in N lowest quantum states

$\Psi_0 = |k_1, \ldots, k_N\rangle$ s.t $\sum \varepsilon_k$ min.

$\Psi_0(r_1 \ldots r_N) = \det\left[\varphi_{k_i}(r_j)\right]$

Slater det (antisymetry)

Excitations

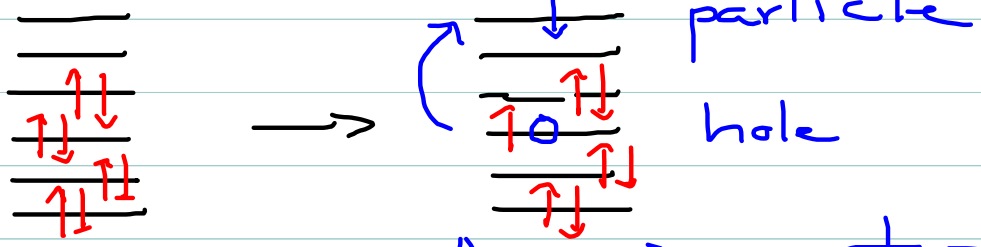

An eigenstate

→ "Elementary excitations" combinations of those yield all eigenstates.

Fermi surface : separating occupied from unocc. states in k-space. ⊤

Low-energy excited states
involve elem. excitations close to FS

FS: $\vec{k}$ / $\varepsilon_{\vec{k}\nu} = \varepsilon_F$ highest occ. energy
can be multi-sheeted in multi-band case.

Fermi energy (metal or liquid):

$$\lim_{T \to 0} \mu(T, n) = \varepsilon_F(n)$$

Interior of FS contains exactly
N 1-p quantum states w/ N = p. number

Ex: N_σ fermions of spin σ in volume Ω
in free space.

$$N_\sigma = \sum_{\vec{k}\,;\,\varepsilon_k < \varepsilon_F} = \frac{\Omega}{(2\pi)^3} \frac{4}{3} \pi k_F^3$$

$$\longrightarrow n_\sigma \equiv \frac{N_\sigma}{\Omega} = \frac{1}{6} \left(\frac{k_F}{\pi} \right)^3$$

Density of states

Define, for a given band and spin component:

$$D_{\nu\sigma}(\varepsilon) = \int_{BZ} \frac{d\vec{k}}{V_{BZ}} \delta(\varepsilon - \varepsilon_{\nu\sigma\vec{k}})$$

Normalized s.t. $\int_{-\infty}^{\hat{\infty}} d\varepsilon \, D_{\nu\sigma} = 1$

Calculation of <u>extensive</u> qty such as:

$$\Phi_{\nu\sigma} \equiv \sum_{\vec{k}\in BZ} \phi(\varepsilon_{\vec{k}\nu\sigma})$$

$$\sum_{k\in BZ} = \frac{\Omega}{(2\pi)^d} \int_{BZ} d\vec{k} = \frac{\Omega V_{BZ}}{(2\pi)^d} \int_{BZ} \frac{d\vec{k}}{V_{BZ}}$$

And for 1 atom / unit-cell of lattice:

$\Omega = N_{at} \cdot V_{cell}$ $\quad V_{cell} \cdot V_{BZ} = (2\pi)^d$

$$\longrightarrow \boxed{\Phi_{\nu\sigma} = N_{at} \int d\varepsilon \, D_{\nu\sigma}(\varepsilon) \phi(\varepsilon)}$$

Thermodynamics of free fermions

Grand-canonical potential:

$$\frac{A}{N_{at}} = -kT \int d\varepsilon \, \mathcal{D}(\varepsilon) \ln\left[1+e^{-\beta(\varepsilon-\mu)}\right]$$

with $\mathcal{D}(\varepsilon) = \sum_{\nu\sigma} D_{\nu\sigma}(\varepsilon)$ total d.o.s

$$\frac{N}{N_{at}} = \int d\varepsilon \, \mathcal{D}(\varepsilon) f(\varepsilon) \quad ; \quad f(\varepsilon) = \underset{\text{Fermi}}{\left[1+e^{-\beta(\varepsilon-\mu)}\right]^{-1}}$$

Per atom:

[Ex0] $C = \frac{\pi^2}{3} k_B \, \mathcal{D}(\varepsilon_F) . k_B T \quad T \ll \varepsilon_F / k_B$

$\chi \sim \frac{(g\mu_B)^2}{4} \mathcal{D}(\varepsilon_F)$ Pauli

$\chi \sim \frac{\partial N}{\partial \mu} \sim \mathcal{D}(\varepsilon_F)$ compressibility.

Technical stuff ...

1. "Second" Quantization : basics

$|\alpha\rangle$ labels 1-particle state e.g. $\alpha = \{\vec{k}, \sigma, \nu, \dots\}$

1-particle wave-function $\varphi_\alpha(1) = \langle 1|\alpha\rangle$

(1 = coordinates of particle 1)

2-particle states (fermions → antisymmetry)

$$\psi_{\alpha\beta}(1,2) = \frac{1}{\sqrt{2}}\left[\varphi_\alpha(1)\varphi_\beta(2) - \varphi_\alpha(2)\varphi_\beta(1)\right]$$

N-particle : Slater determinant

$$\psi_{\alpha_1\dots\alpha_N}(1,\dots,N) = \frac{1}{\sqrt{N!}}\sum_{P\in S_N}(-1)^P \varphi_{\alpha_1}(P_1)\cdots\varphi_{\alpha_N}(P_N)$$

Fock space : $\mathcal{H}_N$ antisym. states of N fermions -

Occupation numbers representation :

$|n_{\alpha_1}\dots n_{\alpha_N}\rangle$ represents $|\psi_{\alpha_1\dots\alpha_N}\rangle$

with $n_\alpha = 1$ for $\alpha = \alpha_i \quad i = 1\dots N$

$$|n_{\alpha_1}\dots n_{\alpha_N}\rangle = |0\dots \overset{\alpha_1}{1}\dots 0\dots \overset{\alpha_2}{1}\dots 0\dots(\dots)\overset{\alpha_N}{1}\rangle$$ ordering of states required

Creation operators :

$$|\alpha\rangle = c_\alpha^+|\text{vac.}\rangle \qquad |\alpha,\beta\rangle = c_\alpha^+ c_\beta^+|\text{vac}\rangle \text{ in } \mathcal{H}_2$$

$$|\alpha_1\dots\alpha_N\rangle = c_{\alpha_1}^+\dots c_{\alpha_N}^+|\text{vac}\rangle$$

Antisymmetry is insured by:

$$\{c_\alpha, c_\beta\} = 0 \qquad \{c_\alpha, c_\beta^+\} = \delta_{\alpha\beta}$$

$$c_\alpha^+ |\{n_\beta\}\rangle = 0 \text{ if } n_\alpha = 1$$
$$= (-1)^{\sum_{\beta<\alpha} n_\beta} |n_1 n_2 \ldots 1^{\downarrow \alpha} n_{\alpha+1} \ldots n_N\rangle$$

2-Representation of 1-body operators

$\hat{O}^{(1)} = \sum_{i=1}^{N} \hat{\omega}^{(1)}[i]$ i denotes i-th particle.

Insert complete set of 1P states $\sum_\alpha |\alpha\rangle\langle\alpha| = \mathbb{1}$ in $\mathcal{H}_1$

$\hat{\omega} = \sum_{\alpha\beta} |\alpha\rangle\langle\alpha|\hat{\omega}|\beta\rangle\langle\beta|$ acts in $\mathcal{H}_1$

$$\hat{O}^{(1)} = \sum_{\alpha\beta} \langle\alpha|\hat{\omega}|\beta\rangle\, c_\alpha^+ c_\beta \quad \text{in } \mathcal{H}_N$$

Note $\langle\alpha|\hat{\omega}|\beta\rangle = \int d\underline{1}\, d\underline{2}\, \varphi_\alpha^*(1) \langle 1|\hat{\omega}|2\rangle \varphi_\beta(2)$

Examples – 1 body

Kinetic energy: 1P w.f. $\varphi_{\vec{k}\sigma\nu}$, $\varepsilon_{\vec{k}\nu\sigma}$ diagonalize K.E

$$\hat{H}_0 = \sum_{\vec{k}\sigma\nu} \varepsilon_{\vec{k}\nu\sigma}\, c_{\vec{k}\sigma\nu}^+ c_{\vec{k}\sigma\nu}^+$$

Continuum: $\sum_{\vec{k}\sigma} \frac{\hbar^2 k^2}{2m} c_{\vec{k}\sigma}^+ c_{\vec{k}\sigma} = \Omega \int \frac{d^3k}{(2\pi)^3} \frac{\hbar^2 k^2}{2m} \sum_\sigma c_{\vec{k}\sigma}^+ c_{\vec{k}\sigma}$

Solid: $\Omega = N_s \cdot V_{cell}$ w/ N_s: number of sites (cells) in system

V_{cell}: unit-cell volume

$$\sum_{\vec{k}} \to N_s \frac{V_{cell} \cdot V_{BZ}}{(2\pi)^3} \int \frac{d^3k}{V_{BZ}} \dots$$

Since $V_{cell} \cdot V_{BZ} = (2\pi)^3$ we get the K.E operator per lattice site as:

$$\frac{1}{N_s} \hat{H}_0 = \int_{BZ} \frac{d^3k}{V_{BZ}} \sum_{\nu\sigma} \varepsilon_{k\nu\sigma} c^+_{k\sigma\nu} c_{k\sigma\nu}$$

Density operator (1-body):

$$\hat{\rho}(r) = \sum_i \delta(\hat{r} - \hat{r}_i) \quad \hat{\omega} = |r\rangle\langle r| \quad \langle\alpha|\hat{\omega}|\beta\rangle = \varphi^*_\alpha(r)\varphi_\beta(r)$$

$$\hat{\rho}(r) = \sum_{\alpha\beta} \varphi^+_\alpha(r)\varphi_\beta(r)\, c^+_\alpha c_\beta \equiv \psi^+(r)\psi(r)$$

Continuum: $\varphi_{\vec{k}}(r) = \frac{1}{\sqrt{\Omega}} e^{i\vec{k}\cdot\vec{r}}$

$$\left|\frac{1}{\sqrt{\Omega}}\right|^2 \sum_{kk'} e^{-i\vec{r}\cdot(\vec{k}-\vec{k}')} c^+_k c_{k'}$$

Fourier comp. $\hat{\rho}_q = \int dr\, e^{-iq\cdot r} \hat{\rho}(r)$

$$\int dr\, e^{-ir[k-k'+q]} = \Omega\, \delta_{k',k+q}$$

$$\to \hat{\rho}_q = \sum_k c^+_k c_{k+q} = \sum_k c^+_{k-q} c_k$$

Ex: Generalize this to lattice

$$\hat{\rho}_q = \sum_{k;\nu\nu'} R^{\nu\nu'}_{kq}\, c^+_{k-q,\nu} c_{k\nu'} \quad R: \text{form factor}.$$

Two-particle operators

$$\hat{O}_2 = \frac{1}{2} \sum_{i \neq j} \hat{\omega}^{(2)}[i,j]$$

$$= \frac{1}{2} \sum_{\alpha\beta\gamma\delta} \langle \alpha\beta | \hat{\omega} | \gamma\delta \rangle \, c_\alpha^+ c_\beta^+ c_\delta c_\gamma$$

2 Note ordering!

$$\langle \alpha\beta | \hat{\omega} | \gamma\delta \rangle = \int d\underline{1}\, d\underline{2}\; \varphi_\alpha^*(1) \varphi_\beta^*(2) \omega[1,2] \varphi_\gamma(1) \varphi_\delta(2)$$

Proof: $\hat{O} = \frac{1}{2} \int d\underline{1} d\underline{2}\; \hat{\rho}(1) \hat{\rho}(2) \omega[1,2]$

$$- \frac{1}{2} \int d\underline{1}\; \omega[1,1] \hat{\rho}(1) \quad \text{assuming } \omega[1,1] \text{ finite}$$

Insert $\hat{\rho}(1) = \sum_{\alpha\beta} \varphi_\alpha^*(1) \varphi_\beta(1) \, c_\alpha^+ c_\beta$

and use $\{c_\alpha, c_\beta^+\} = \delta_{\alpha\beta}$ $\{c_\alpha, c_\beta\} = 0$ □

Interaction $\hat{H}_{int} = \frac{1}{2}\sum_{i\neq j} v(r_i - r_j)$

$$\hat{H}_{int} = \frac{1}{2\Omega}\sum_{k_1 k_2 q}\sum_{\sigma_1\sigma_2} c^+_{k_1+q,\sigma_1} c^+_{k_2-q,\sigma_2} c_{k_2\sigma_2} c_{k_1\sigma_1} \hat{v}(q)$$

Interaction vertex [diag.]:

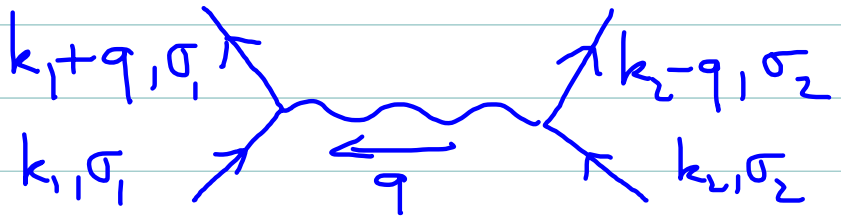

Exercise: prove this !

Note: The factor $\frac{1}{\Omega}$ insures an extensive energy ($\alpha\Omega$), but it's not that simple to see directly $\rightarrow$ cf TD1

e.g. 1st order terms:

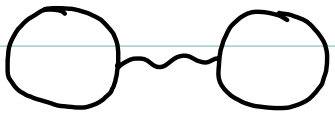

$$\left[\sum_k G(k)\right]^2 \frac{1}{\Omega}\hat{v}(q=0)$$

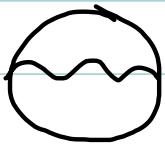

$$\sum_{k,q} \frac{1}{\Omega}\hat{v}(q)\,G(k)\,G(k-q)$$

Both terms: $\sum_k \alpha\Omega$ Hence $\frac{1}{\Omega}\cdot\Omega^2 \propto \Omega$.

Green's functions of all sorts ...

Field operator:

$$\psi(r) \equiv \sum_\alpha \varphi_\alpha(r)\, c_\alpha \;;\; \psi^\dagger(r) = \sum_\alpha \varphi_\alpha^*(r)\, c_\alpha^\dagger$$

Ex: Prove $\{\psi(r), \psi^\dagger(r')\} = \delta(r - r')$

Cont: $\psi_\sigma^\dagger(r) = \frac{1}{\sqrt{\Omega}} \sum_{\vec{k}} e^{-i\vec{k}\cdot\vec{r}}\, c_{k\sigma}^\dagger$

Solid: $\psi_\sigma^\dagger(r) = \sum_{\vec{k}\nu} e^{-i\vec{k}\cdot\vec{r}}\, u_{k\nu}^*(r)\, c_{k\sigma\nu}^\dagger = \sum_{\vec{R}\nu} w_\nu^*(r - R)\, c_{\vec{R}\sigma\nu}^\dagger$

Heisenberg representation

$$\hat{O}(t) = e^{iH't}\, \hat{O}\, e^{-iH't} \qquad \hat{H}' \equiv \hat{H} - \mu \hat{N}$$

Prove: $i \frac{\partial}{\partial t} \hat{O}(t) = [\hat{O}(t), \hat{H}']$

Equal-time $\{,\}$ relations of $\psi(r,t)$ id. to those of $\psi(r)$

Fourier transforms : conventions

$$f(r) = \int \frac{dk}{(2\pi)^d} \int \frac{d\omega}{2\pi}\, e^{i(\vec{k}\cdot\vec{r} - \omega t)} \hat{f}_{k,\omega}$$

$$\hat{f}_{k,\omega} = \int dr \int dt\; e^{-i(kr - \omega t)} f(r,t)$$

Representation of Heaviside function:

$$-i\,\theta(t) = \int_{-\infty}^{+\infty} \frac{d\omega}{2\pi}\, e^{-i\omega t} \frac{1}{\omega + i0^+}$$

Proof : Cauchy

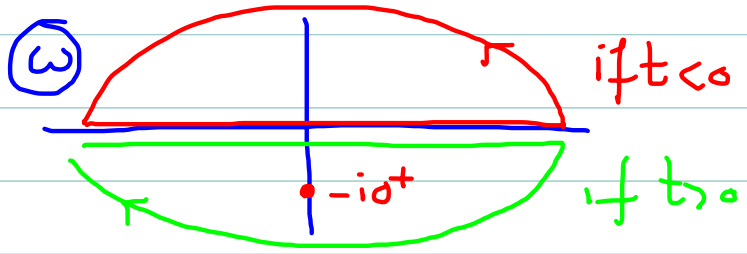

$-i\omega t = -it\,\mathrm{Re}\,\omega + t\,\mathrm{Im}\,\omega$

Hence if $t<0$ must close contour w/ $\mathrm{Im}\,\omega > 0$

$t>0$ " " " w/ $\mathrm{Im}\,\omega < 0$

Sim: $i\,\theta(-t) = \int \frac{d\omega}{2\pi}\, e^{-i\omega t} \frac{1}{\omega - i0^+}$

4 types of Green's functions : spectral repr.

With spectral function $A(\vec{k},\omega)$ defined as:

$$\omega>0: \sum_A |\langle \psi_A | c_k^+ | \psi_0 \rangle|^2 \delta\left[\omega + E_0^N + \mu - E_A^{N+1}\right]$$

$$\omega<0: \sum_B |\langle \psi_B | c_k | \psi_0 \rangle|^2 \delta\left[\omega - E_0^N + \mu + E_B^{N-1}\right]$$

G.F	Spectral
$-i\theta(t)\langle c_k(t) c_k^+(0)\rangle$	$\int_0^\infty d\varepsilon \ \frac{A(k,\varepsilon)}{\omega-\varepsilon+i0^+}$
$i\theta(-t)\langle c_k(t) c_k^+(0)\rangle$	$\int_0^\Delta d\varepsilon \ \frac{A(k,\varepsilon)}{\omega-\varepsilon-i0^+}$
$-i\theta(t)\langle c_k^+(0) c_k(t)\rangle$	$\int_{-\infty}^0 d\varepsilon \ \frac{A(k,\varepsilon)}{\omega-\varepsilon+i0^+}$
$i\theta(-t)\langle c_k^+(0) c_k(t)\rangle$	$\int_{-\infty}^0 d\varepsilon \ \frac{A(k,\varepsilon)}{\omega-\varepsilon-i0^+}$

Retarded G.F (causal)

$$G_R(\vec{k},t) = -i\theta(t)\langle \psi_0 | \{c_{\vec{k}}^+(0), c_k(t)\} | \Psi_0 \rangle$$

$$G_R(\vec{k},\omega) = \int_{-\infty}^{+\infty} d\varepsilon \ \frac{A(\vec{k},\varepsilon)}{\omega-\varepsilon+i0^+}$$

$$A(\vec{k},\omega) = -\frac{1}{\pi} \operatorname{Im} G_R(\vec{k},\omega)$$

Feynman G.F $G_F(\vec{k},t) = -i\langle T_t c_k(t) c_k^+(0)\rangle$

$$G_F(k,\omega) = \int_0^\infty d\varepsilon \ \frac{A(k,\varepsilon)}{\omega-\varepsilon+i0^+} + \int_{-\infty}^0 d\varepsilon \ \frac{A(\vec{k},\varepsilon)}{\omega-\varepsilon-i0^+}$$